

Supporting Information

for

Reversible Nickel-Metallacycle Formation with a Phosphinimine-based Pincer Ligand

Xiujing Xing, Shaoguang Zhang, Laura M. Thierer, Michael R. Gau, Patrick J. Carroll, Neil Tomson*

P. Roy and Diana T. Vagelos Laboratories, Department of Chemistry, University of Pennsylvania, Philadelphia, PA, 19104, United States

Contents

1. NMR Spectra	2
2. Kinetic Study of Isocyanide Insertion.....	25
3. Crystallographic data	32

1. NMR Spectra

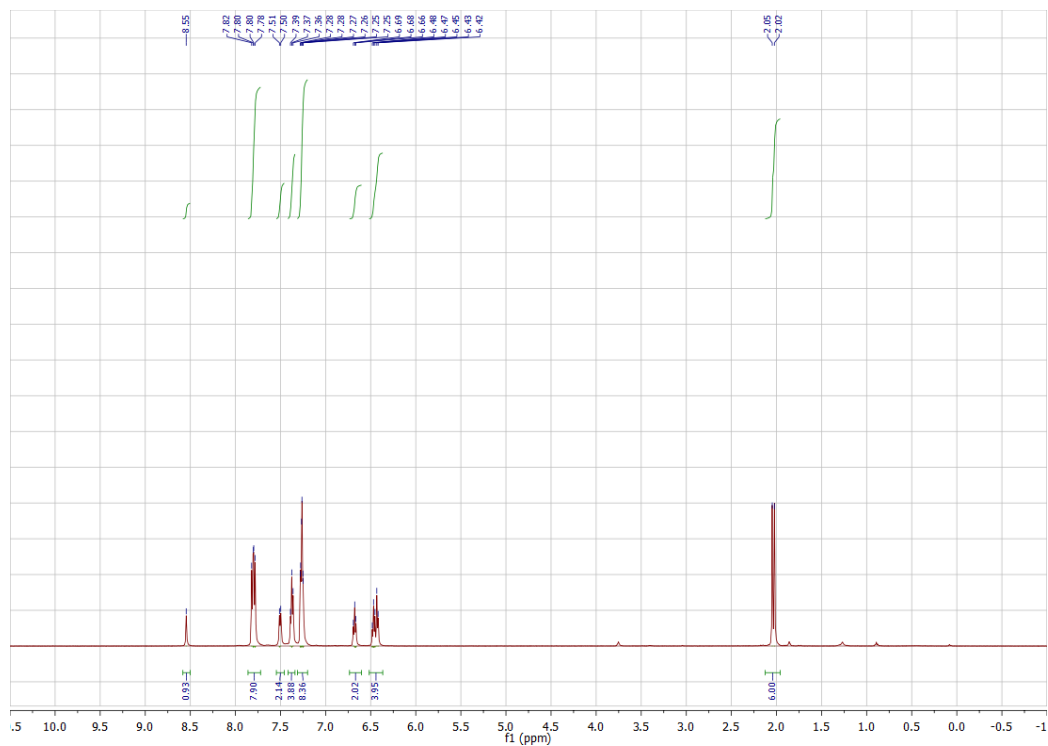


Figure S1. ^1H NMR spectrum of **1** in CDCl_3 .

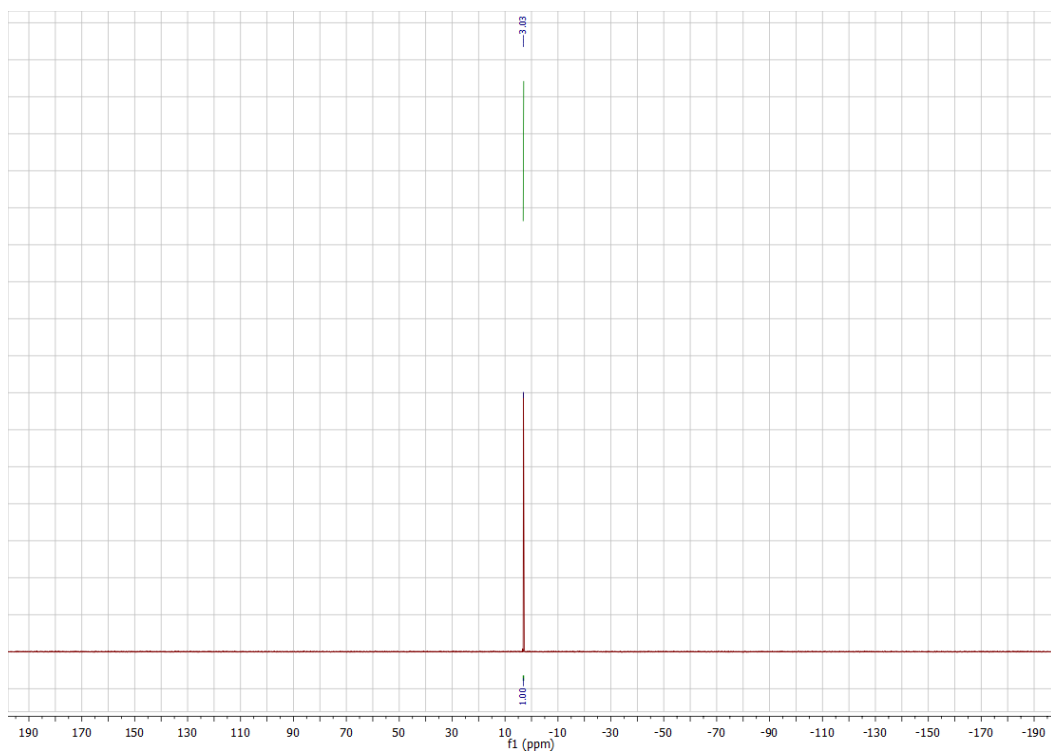


Figure S2. $^{31}\text{P}\{^1\text{H}\}$ NMR spectrum of **1** in CDCl_3 .

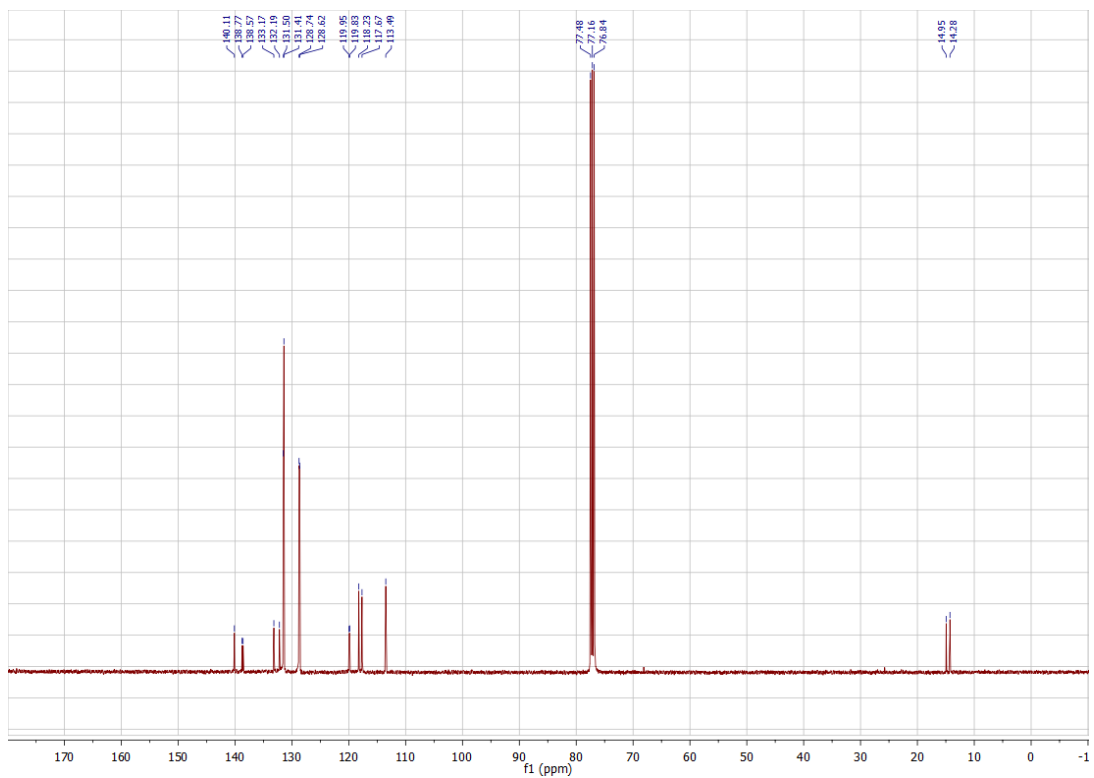


Figure S3. $^{13}\text{C}\{^1\text{H}\}$ NMR spectrum of **1** in CDCl_3 .

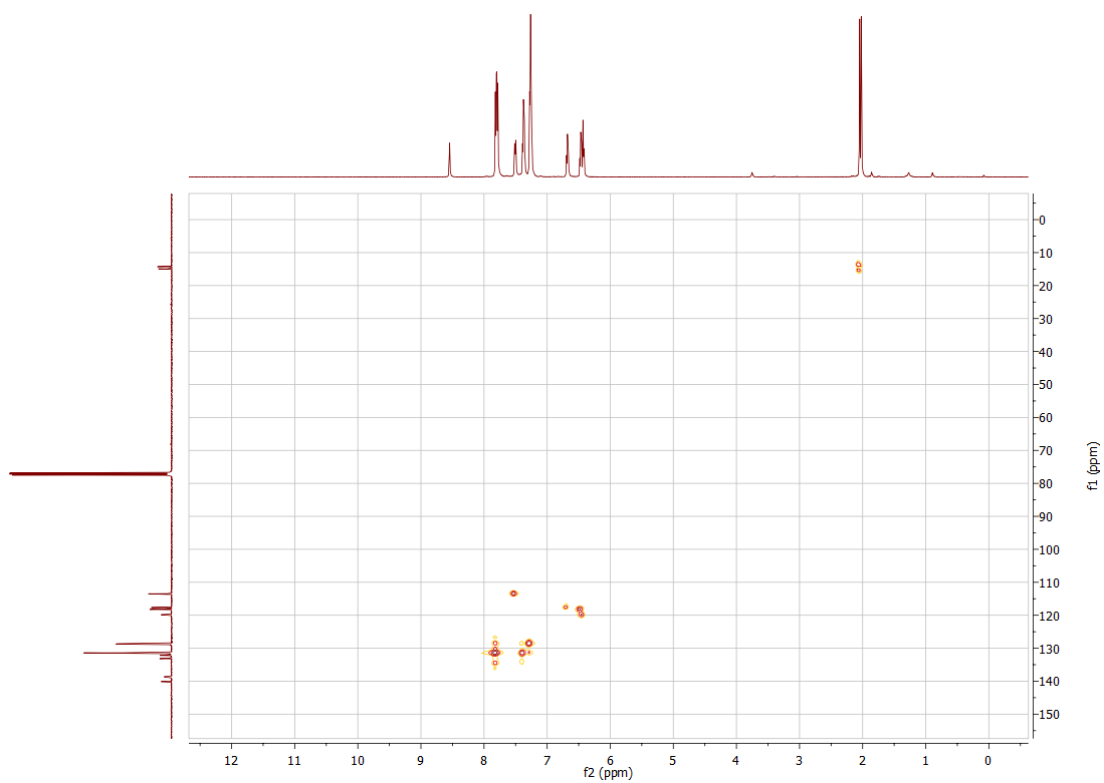


Figure S4. $^1\text{H}-^{13}\text{C}$ HSQC 2D NMR spectrum of **1** in CDCl_3 .

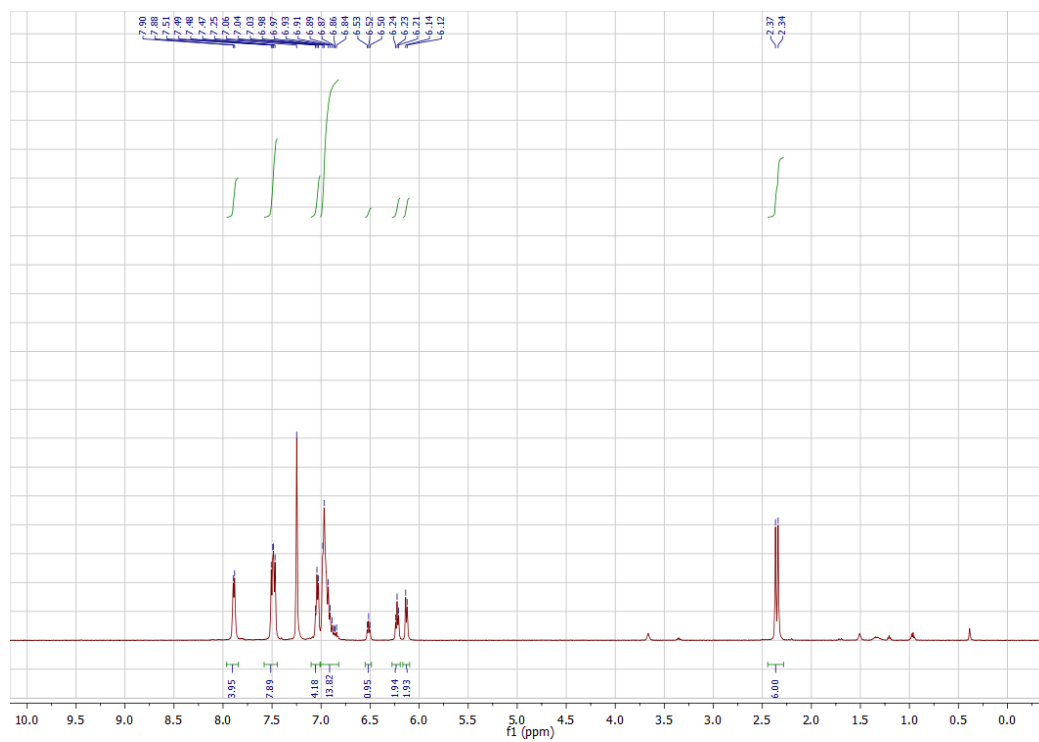


Figure S5. ^1H NMR spectrum of **2** in C_6D_6 .

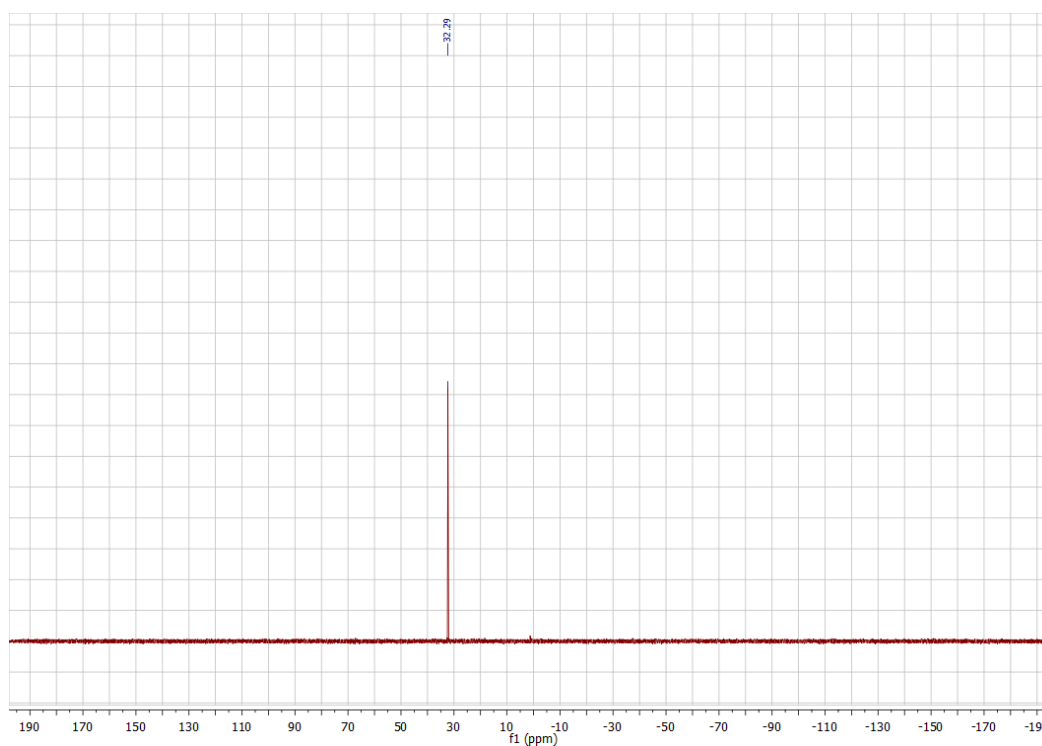


Figure S6. $^{31}\text{P}\{^1\text{H}\}$ NMR spectrum of **2** in C_6D_6 .

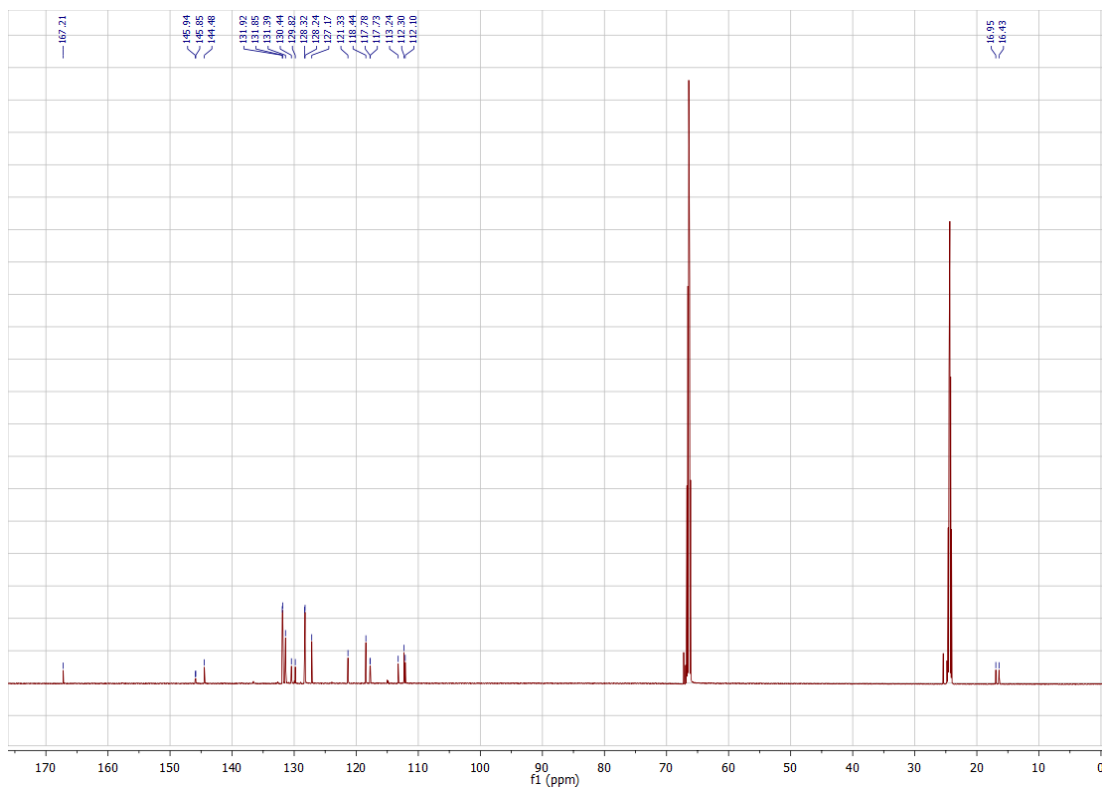


Figure S7. $^{13}\text{C}\{^1\text{H}\}$ NMR spectrum of **2** in $\text{THF-}d_8$.

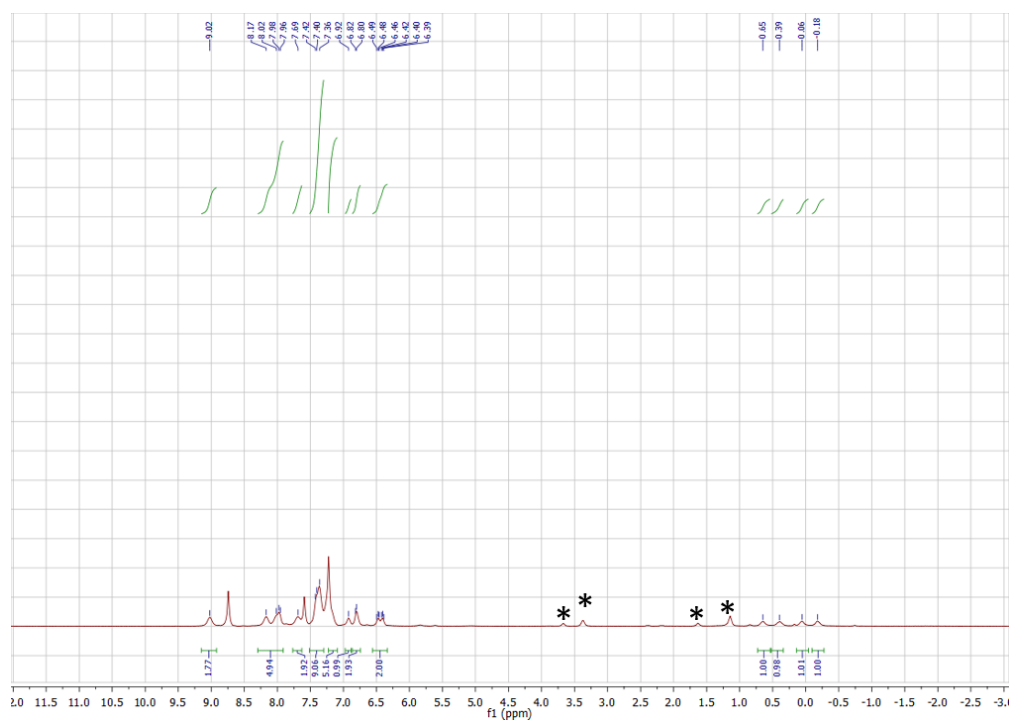


Figure S8. ^1H NMR spectrum of **3** in $\text{Pyr-}d_5$. * = THF and Et_2O .

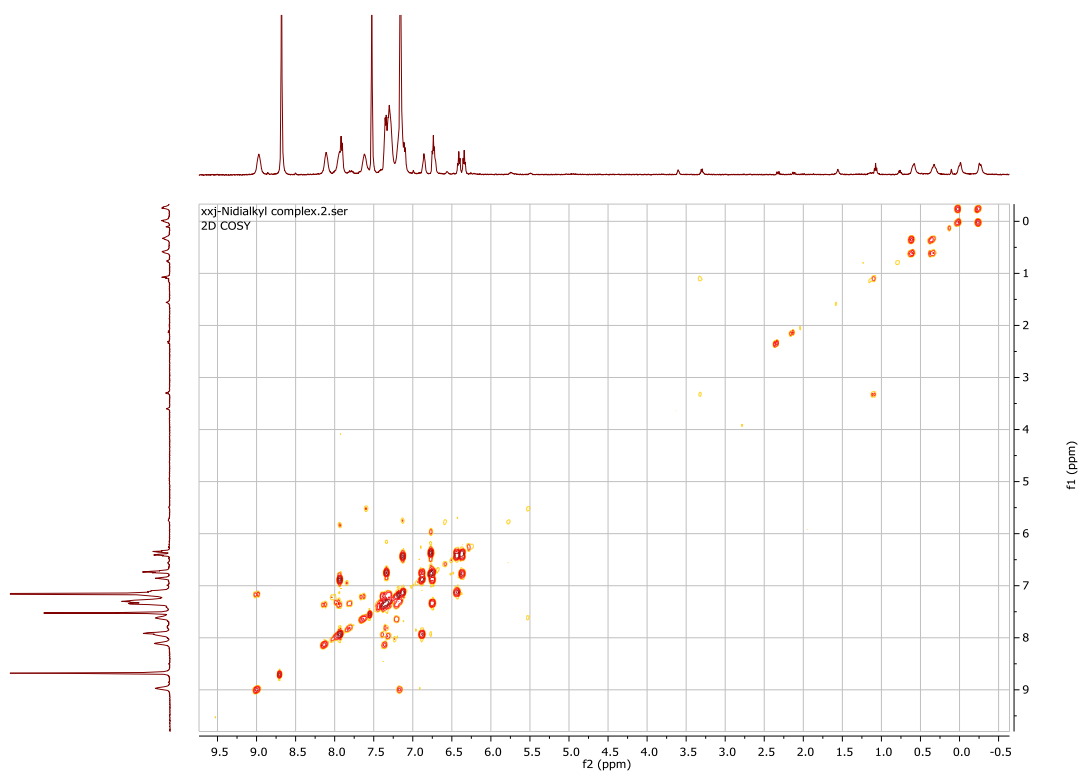


Figure S9. ^1H - ^1H COSY 2D NMR spectrum of **3** in $\text{Pyr-}d_5$.

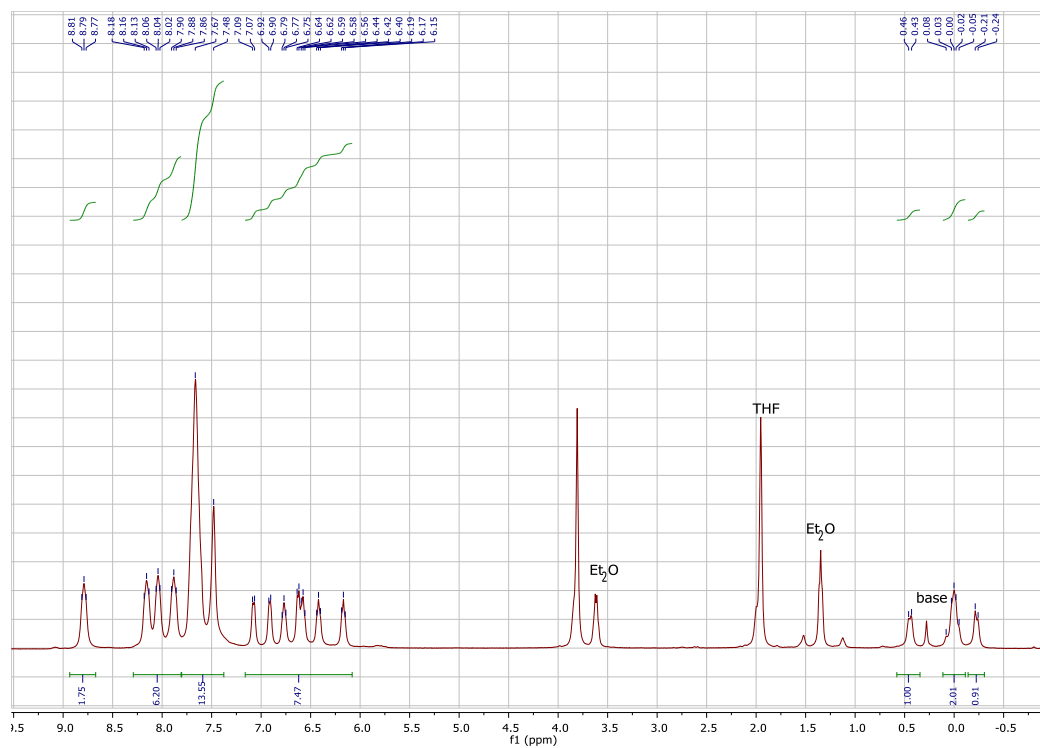


Figure S10. ^1H NMR spectrum of **3** in $\text{THF-}d_8$. Note: Base is NaHMDS.

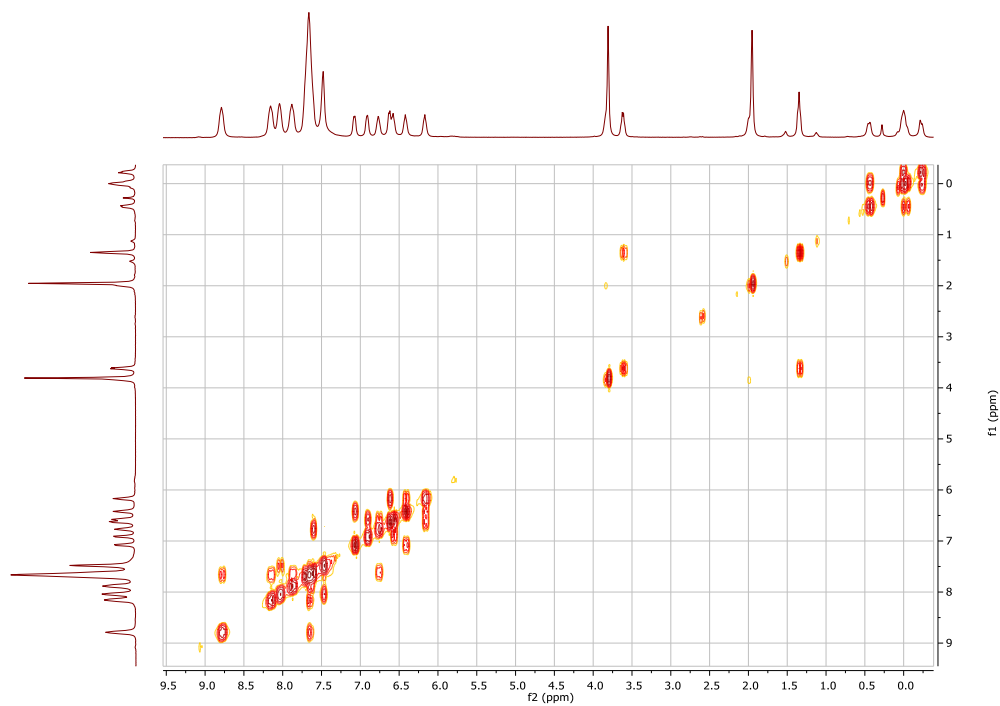


Figure S11. ^1H - ^1H COSY 2D NMR spectrum of **3** in $\text{THF-}d_8$.

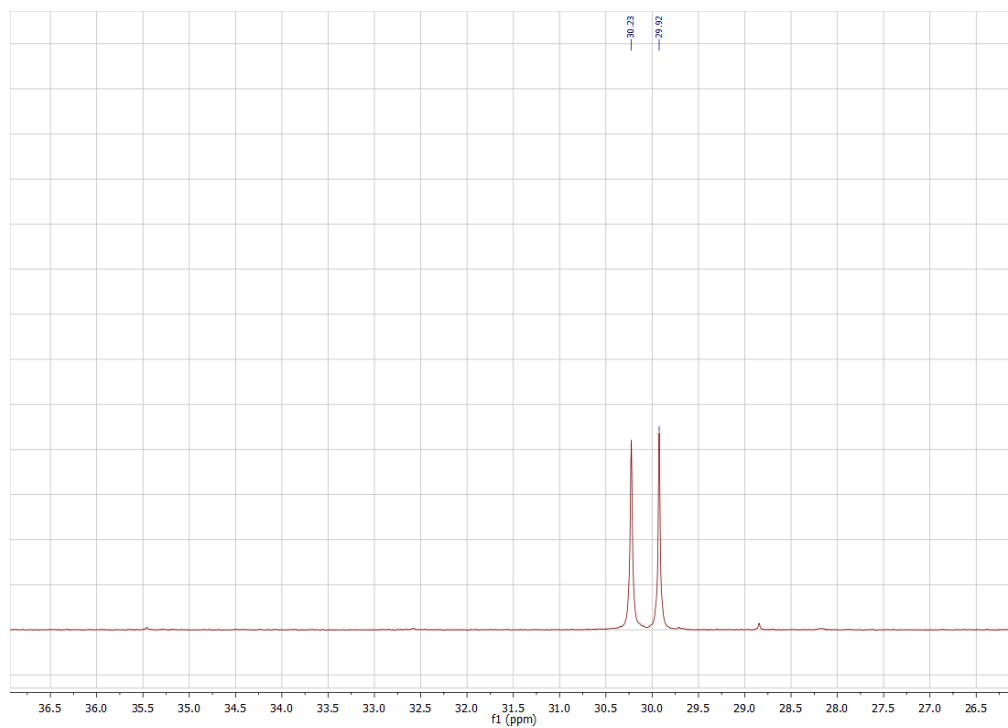


Figure S12. $^{31}\text{P}\{^1\text{H}\}$ NMR spectrum of **3** in $\text{THF-}d_8$.

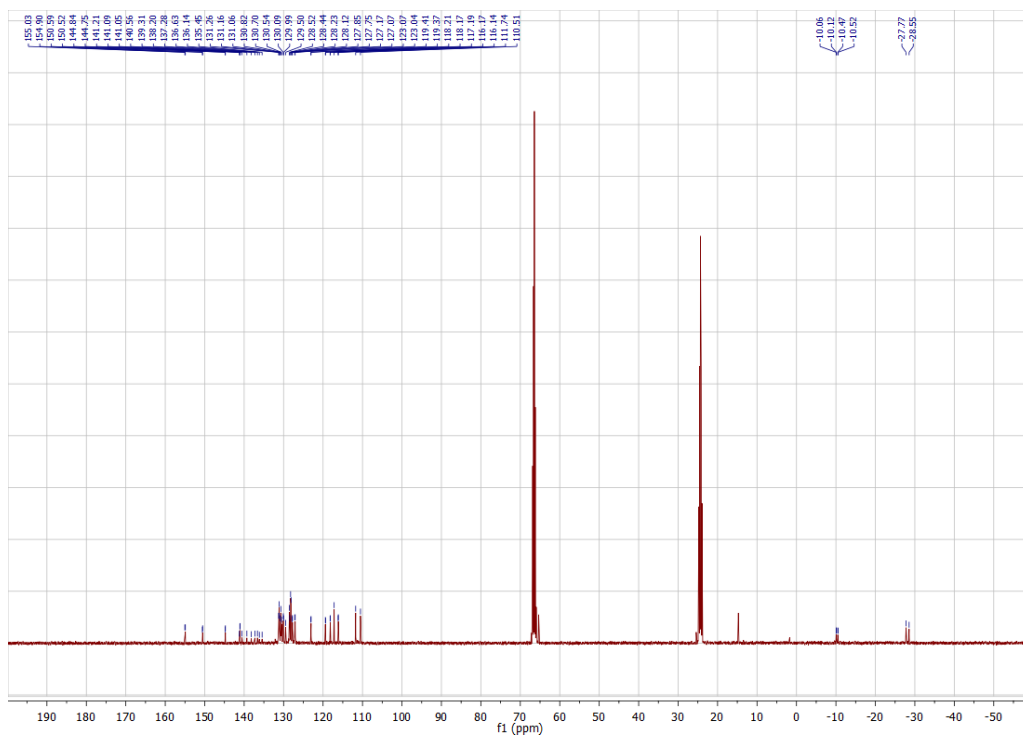


Figure S13a. $^{13}\text{C}\{^1\text{H}\}$ NMR spectrum of **3** in $\text{THF-}d_8$.

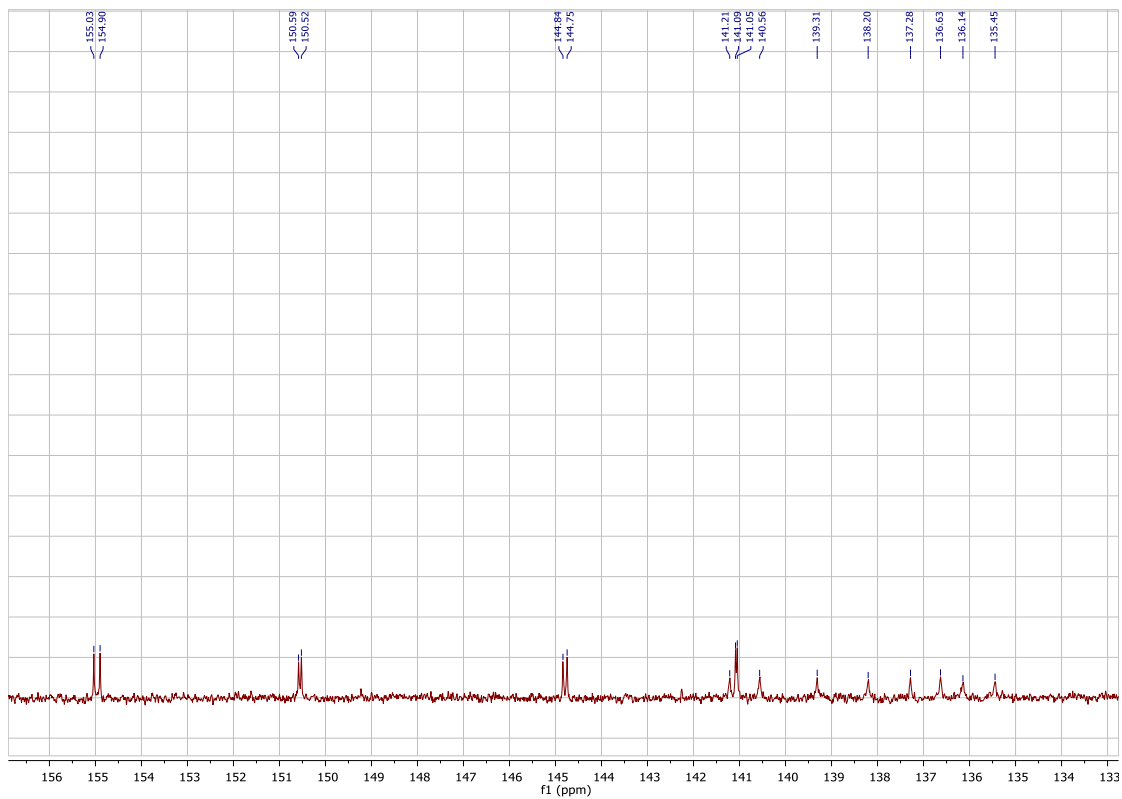


Figure S13b. $^{13}\text{C}\{^1\text{H}\}$ NMR spectrum of **3** in $\text{THF-}d_8$ from 156 to 135 ppm, see Figure S13a for the full spectrum.

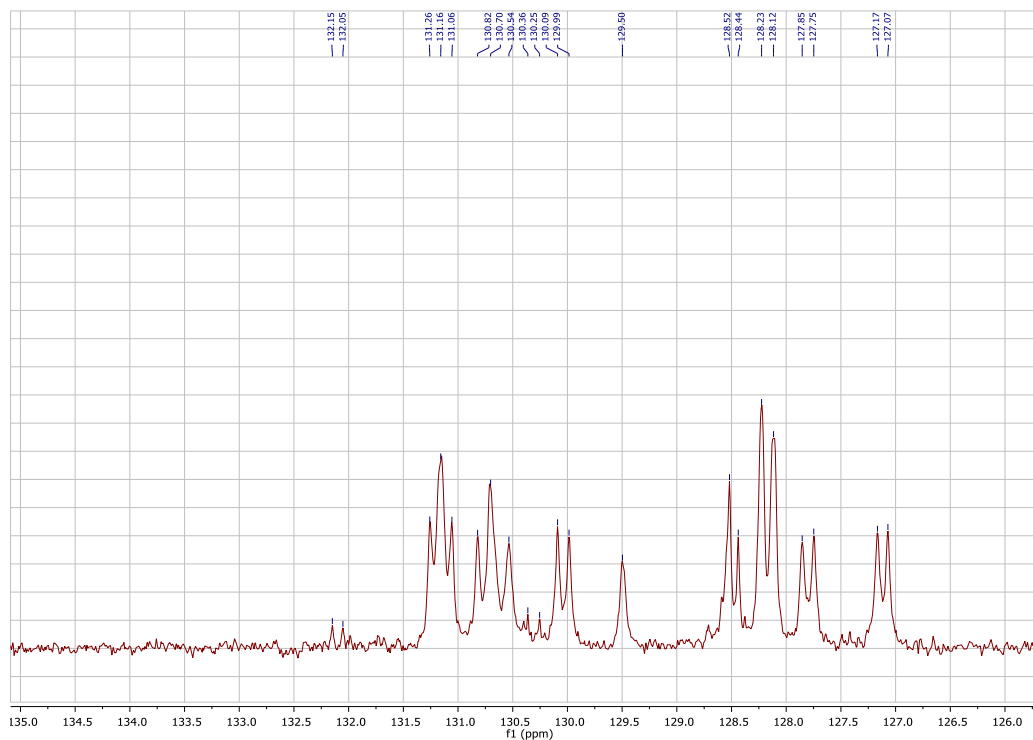


Figure S13c. $^{13}\text{C}\{^1\text{H}\}$ NMR spectrum of **3** in $\text{THF-}d_8$ from 135 to 126 ppm, see Figure S13a for the full spectrum.

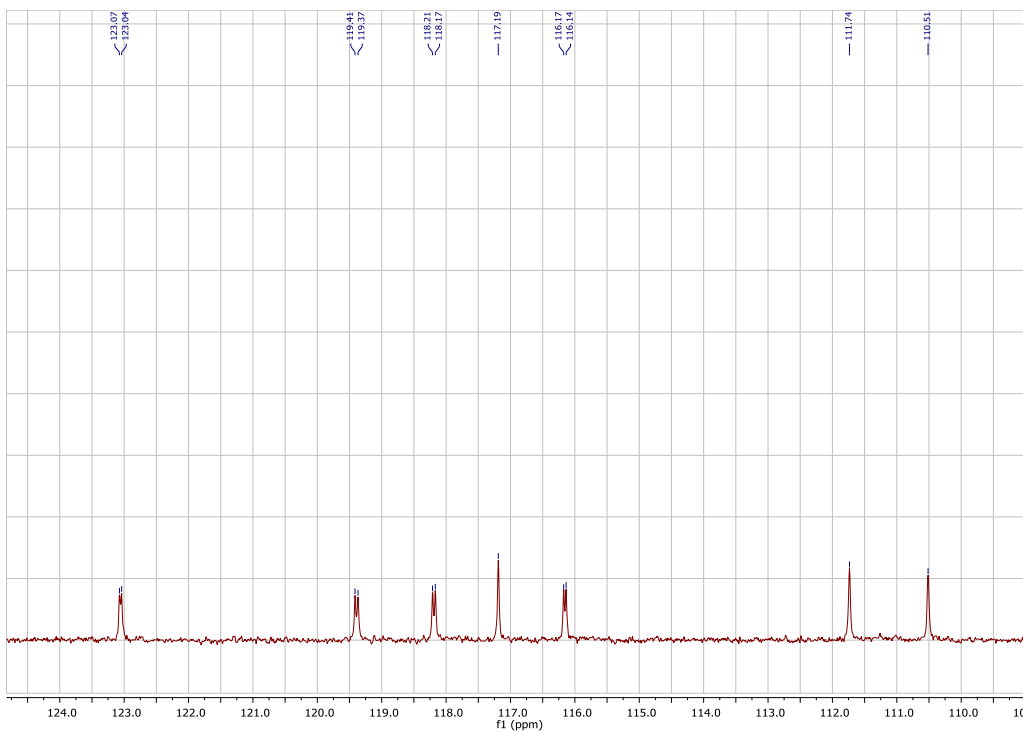


Figure S13d. $^{13}\text{C}\{^1\text{H}\}$ NMR spectrum of **3** in $\text{THF-}d_8$ from 125 to 110 ppm, see Figure S13a for the full spectrum.

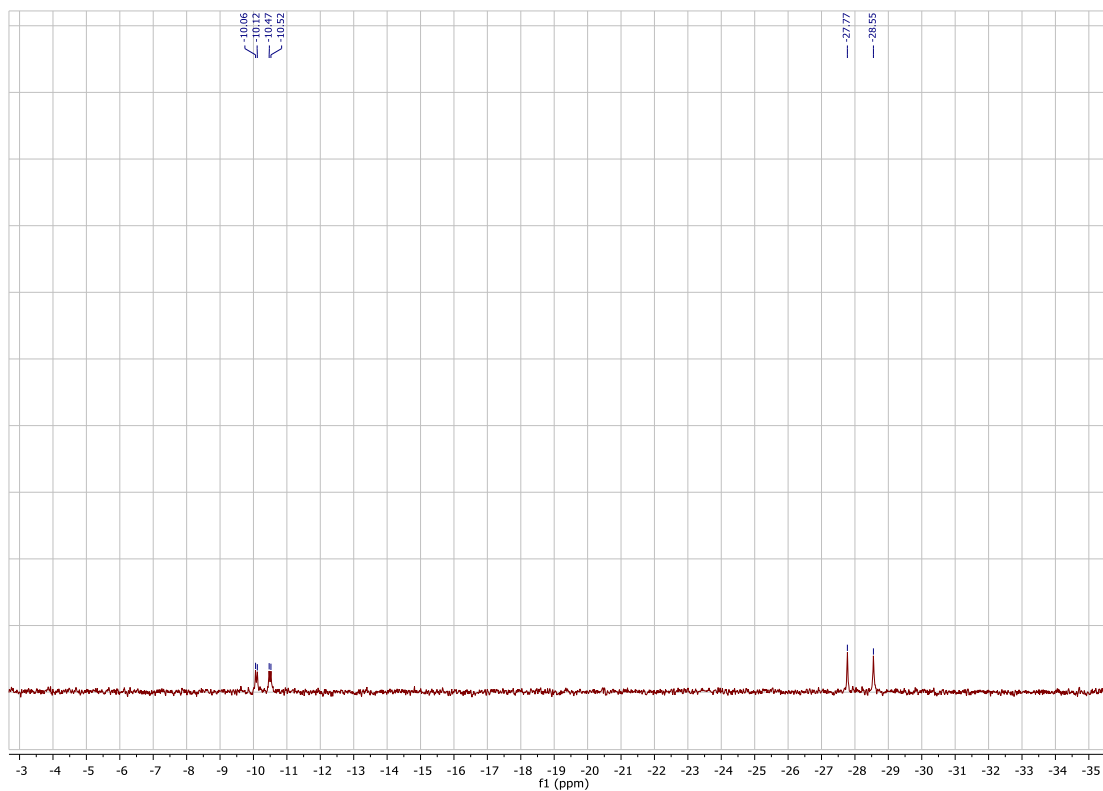


Figure S13e. $^{13}\text{C}\{^1\text{H}\}$ NMR spectrum of **3** in $\text{THF-}d_8$ from -3 to -35 ppm, see Figure S13a for the full spectrum.

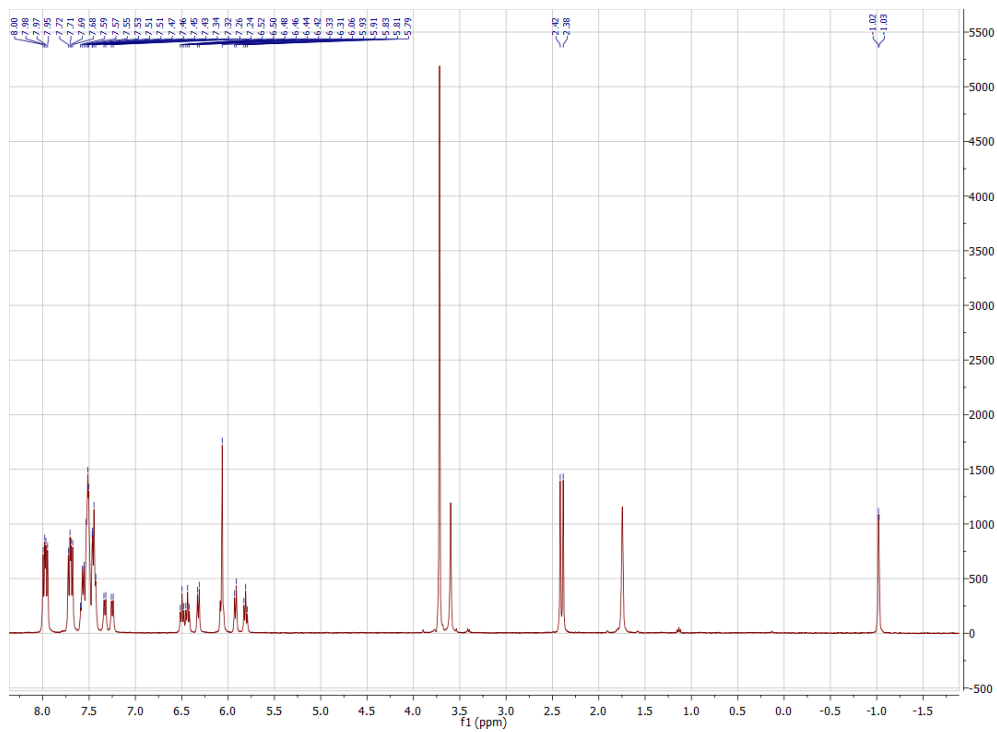


Figure S14. ^1H NMR spectrum of **4** in $\text{THF-}d_8$.

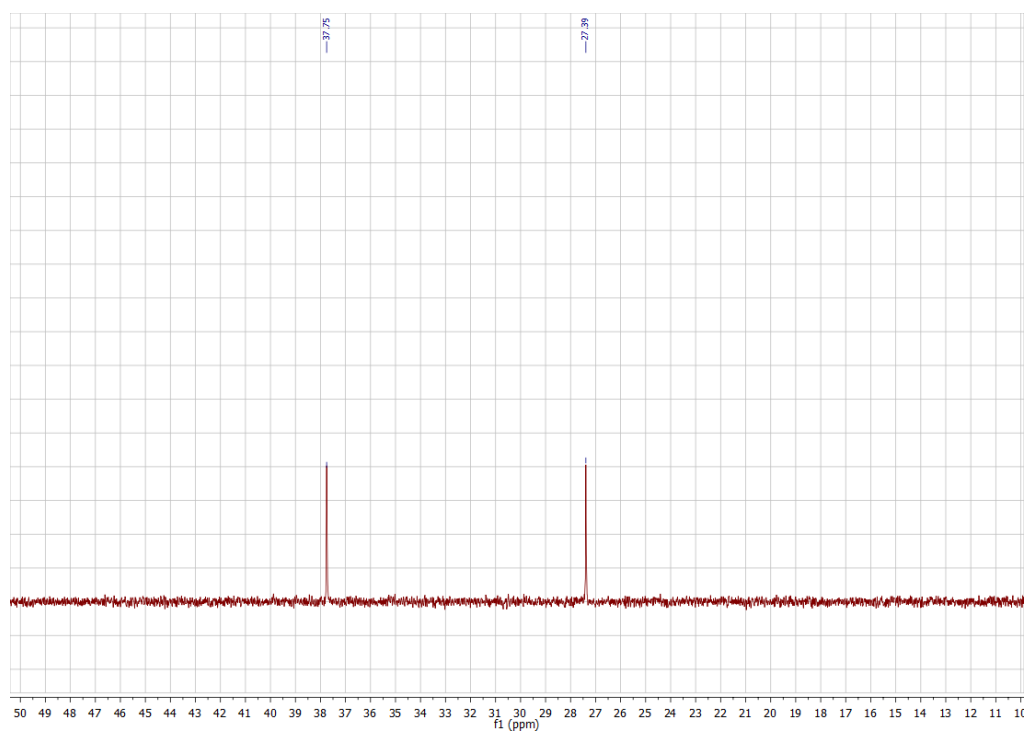


Figure S15. $^{31}\text{P}\{^1\text{H}\}$ NMR spectrum of **4** in C_6D_6 .

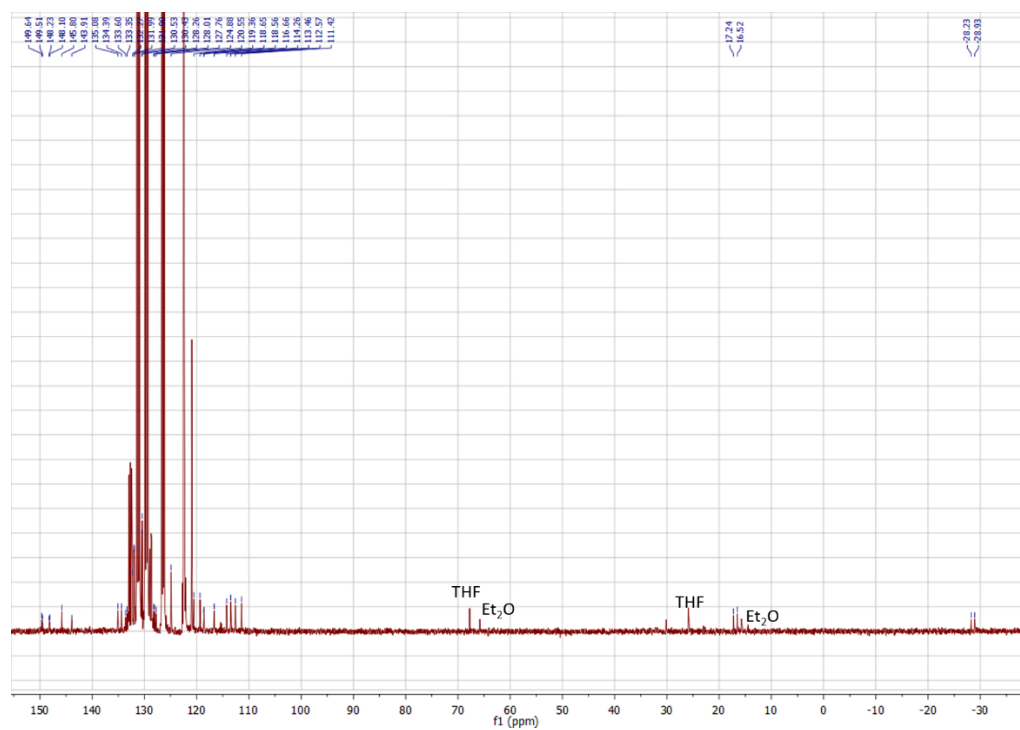


Figure S16a. $^{13}\text{C}\{^1\text{H}\}$ NMR spectrum of **4** in $\text{C}_6\text{D}_5\text{Br}$.

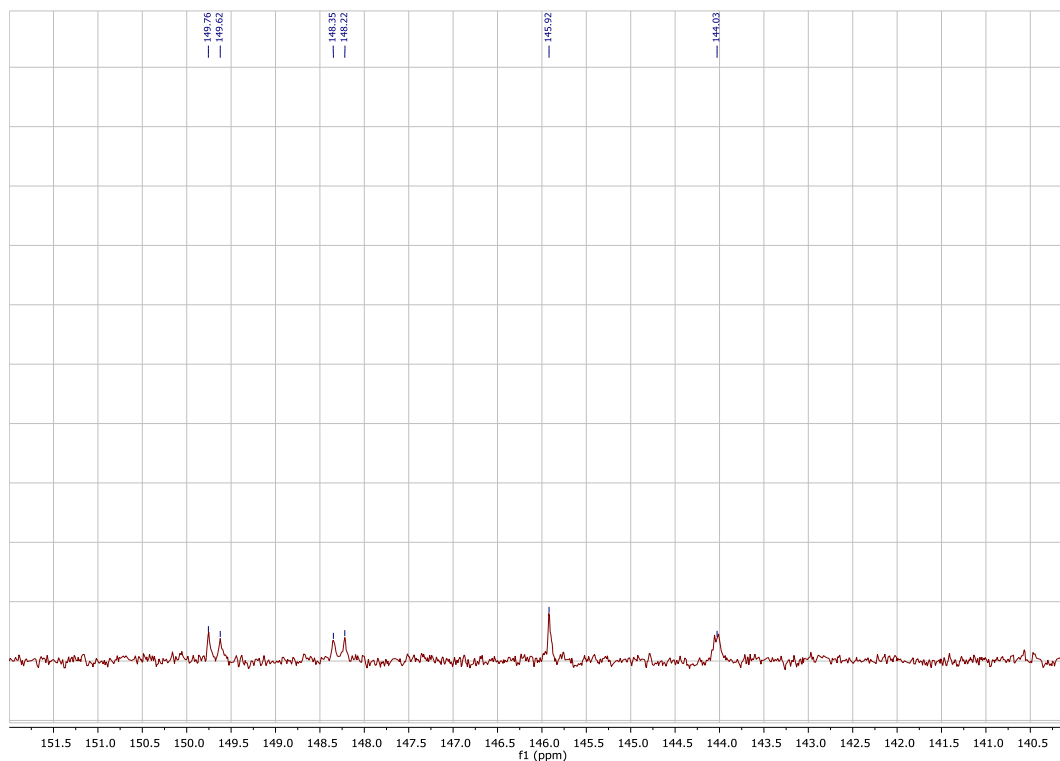


Figure S16b. $^{13}\text{C}\{^1\text{H}\}$ NMR spectrum of **4** in $\text{C}_6\text{D}_5\text{Br}$ from 152 to 140 ppm, see Figure S16a for the full spectrum.

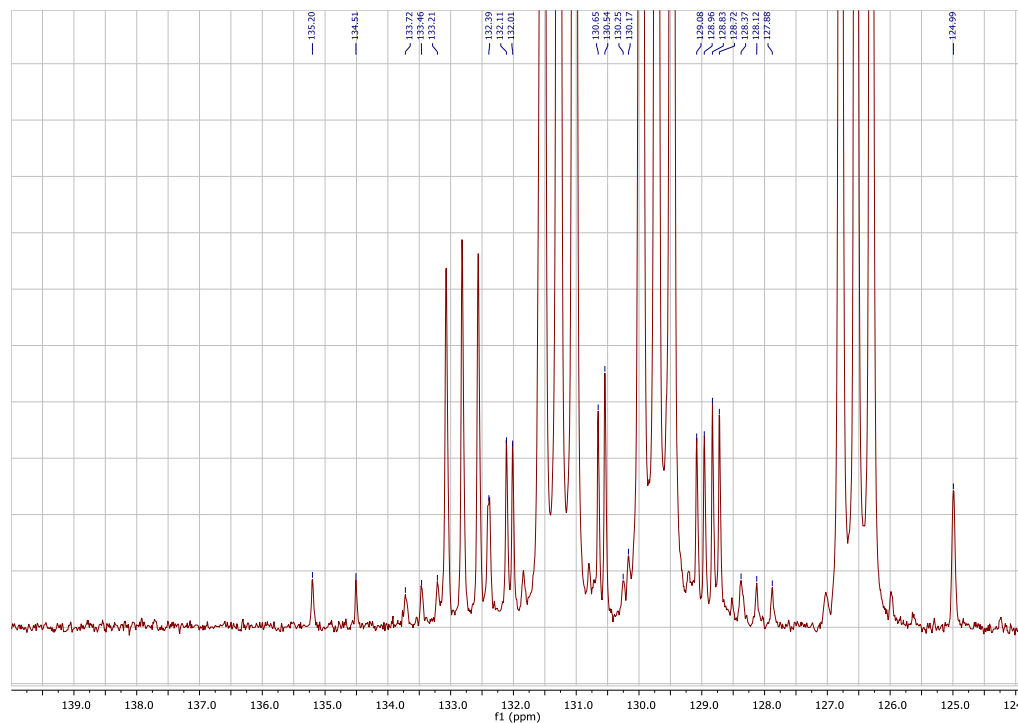


Figure S16c. $^{13}\text{C}\{^1\text{H}\}$ NMR spectrum of **4** in $\text{C}_6\text{D}_5\text{Br}$ from 140 to 124 ppm, see Figure S16a for the full spectrum. Note: 133.09 – 133.60 ppm and 127.76 – 128.26 ppm are solvent residues.

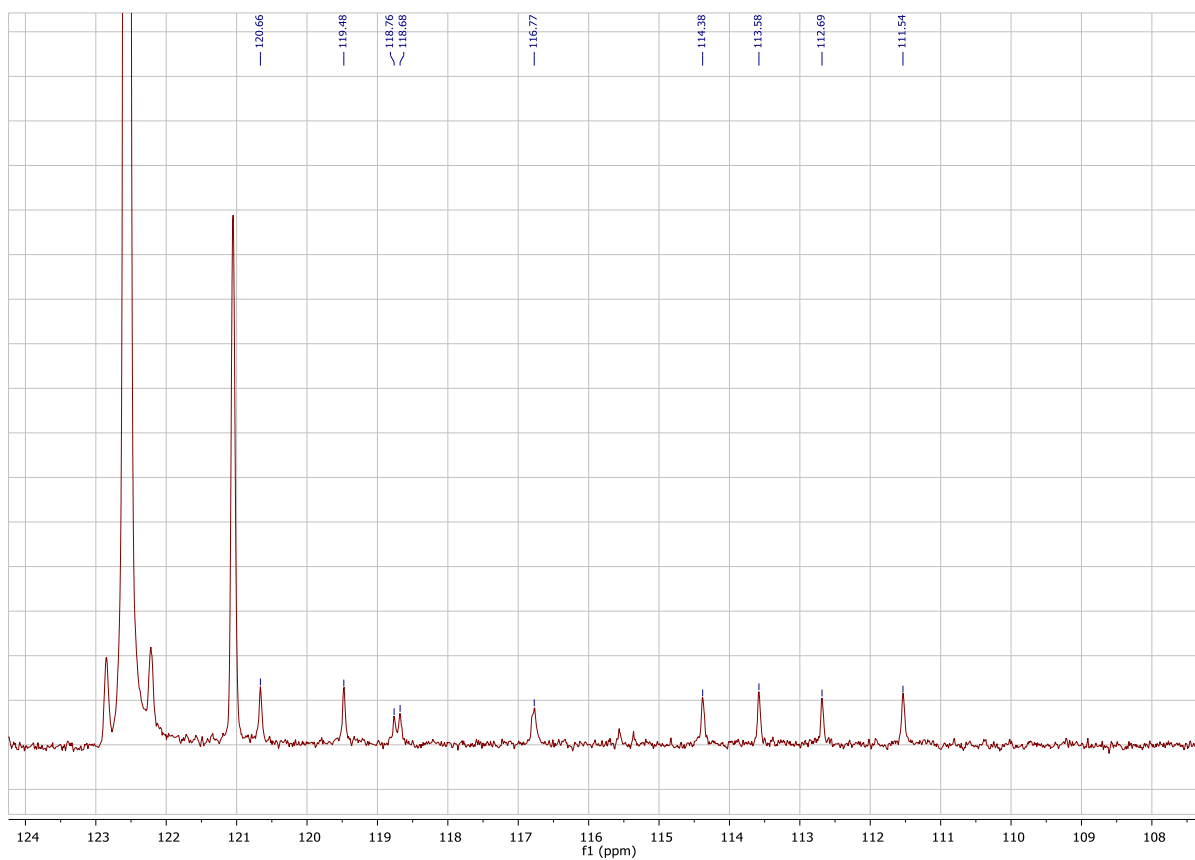


Figure S16d. $^{13}\text{C}\{^1\text{H}\}$ NMR spectrum of **4** in $\text{C}_6\text{D}_5\text{Br}$ from 124 to 106 ppm, see Figure S16a for the full spectrum.

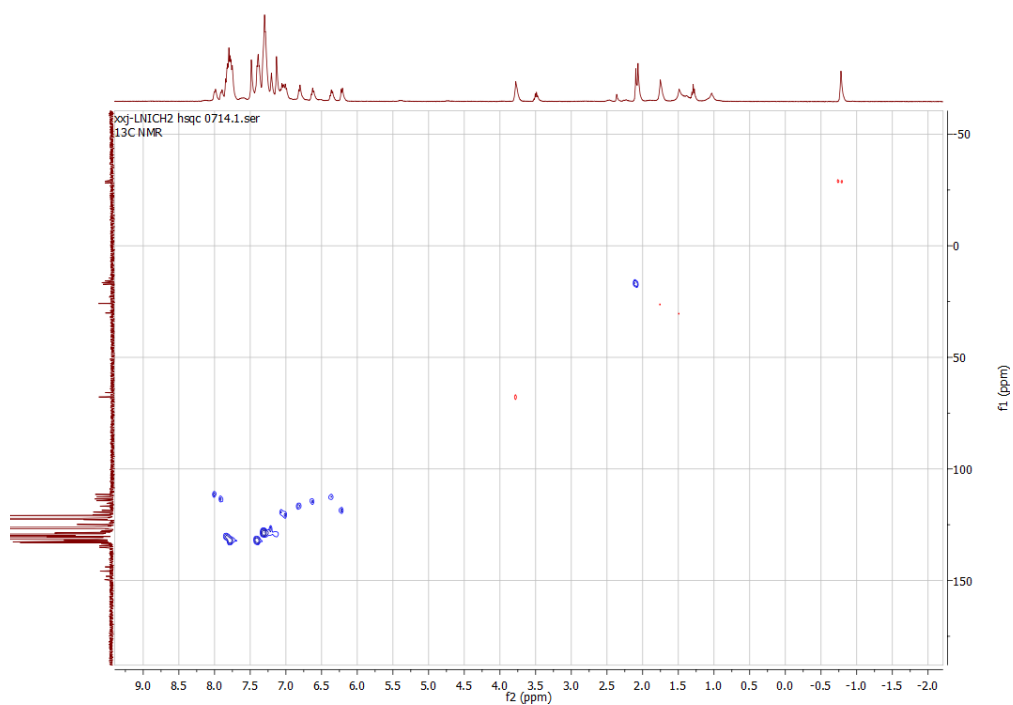


Figure S17. $^1\text{H}-^{13}\text{C}$ HSQC 2D NMR spectrum of **4** in $\text{C}_6\text{D}_5\text{Br}$.

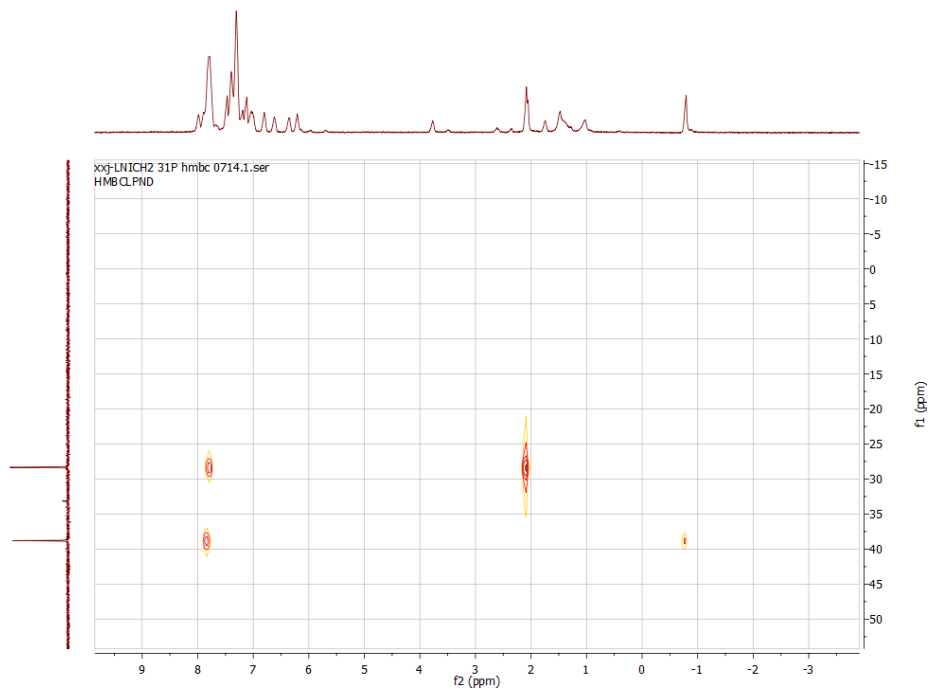


Figure S18. ^1H - ^{31}P HMBC 2D NMR spectrum of **4** in $\text{C}_6\text{D}_5\text{Br}$.

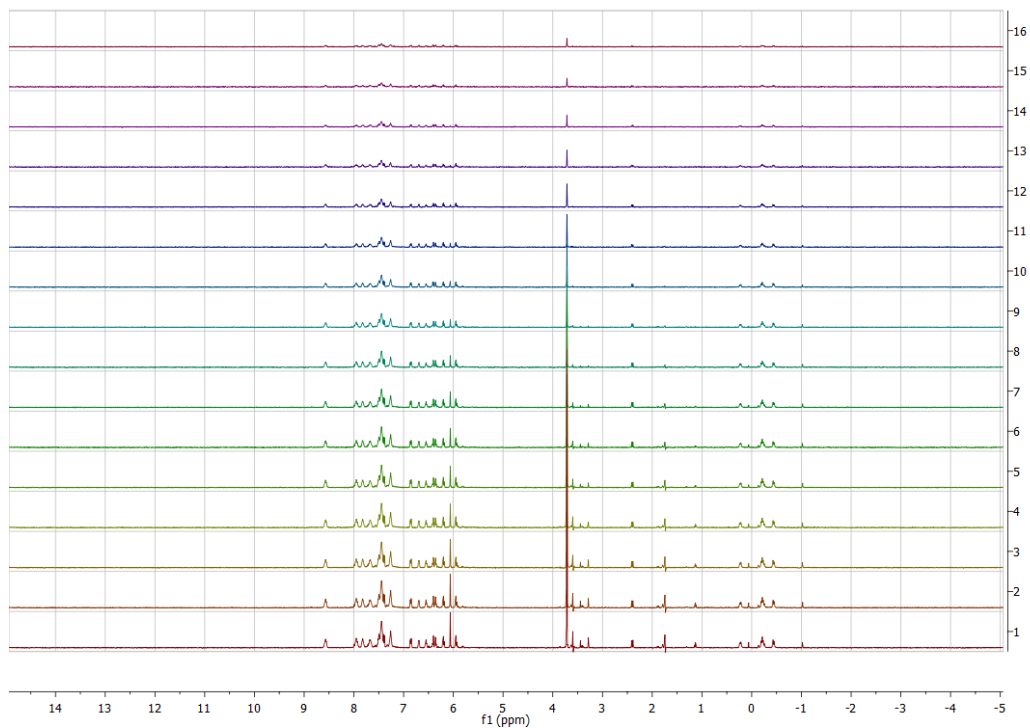


Figure S19. ^1H NMR DOSY spectra of **3** in pyridine- d_5 with different gradients (from 2% to 95%).

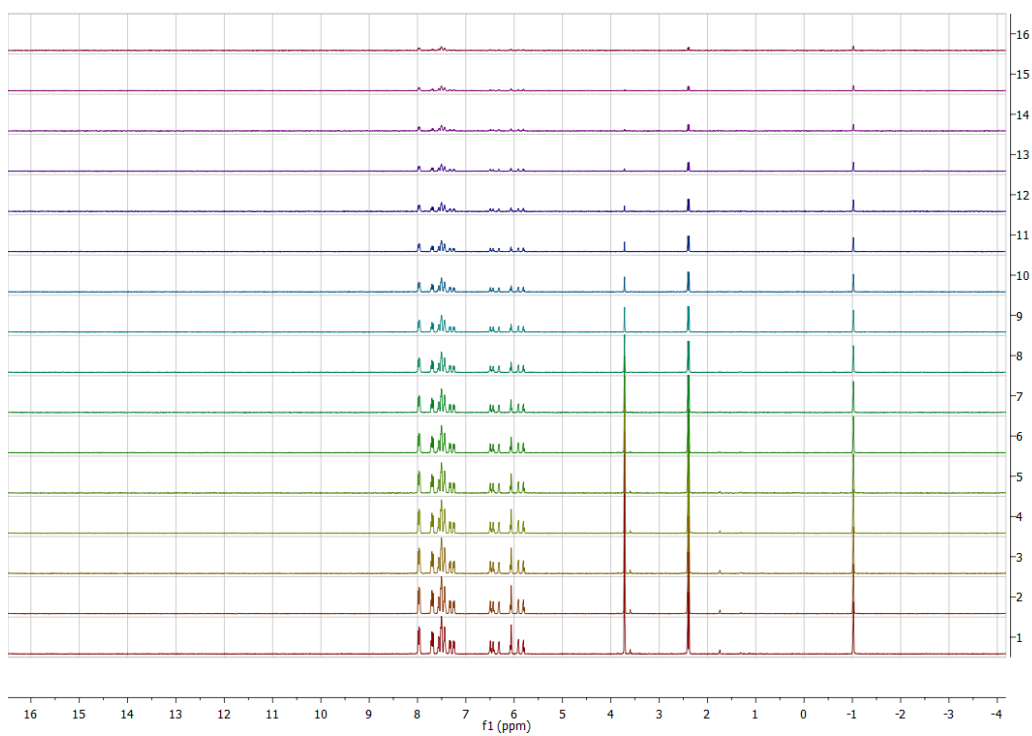


Figure S20. ^1H NMR DOSY spectra of **4** in pyridine- d_5 with different gradients (from 2% to 95%).

Table S21. Diffusion constants obtained from DOSY experiments.

Compound	Diff Constant (m^2/s)
trimethoxybenzene	1.635e-009
3	7.195e-010
4	6.968e-010

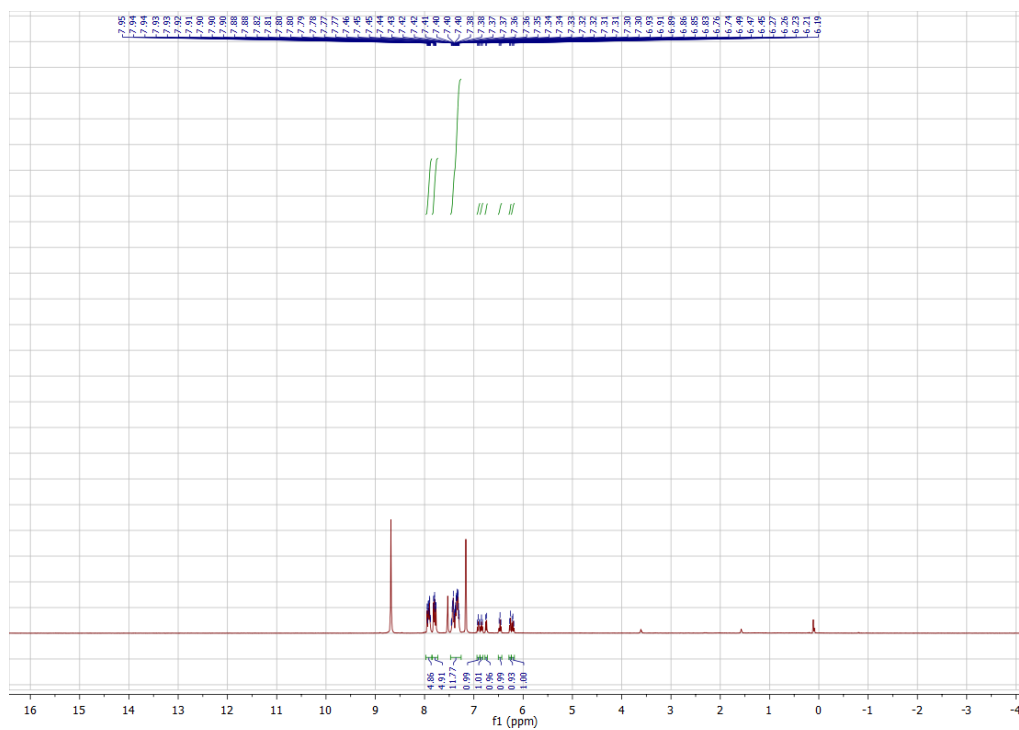


Figure S22. ^1H NMR spectrum of $4-d_5$ in pyridine- d_5 .

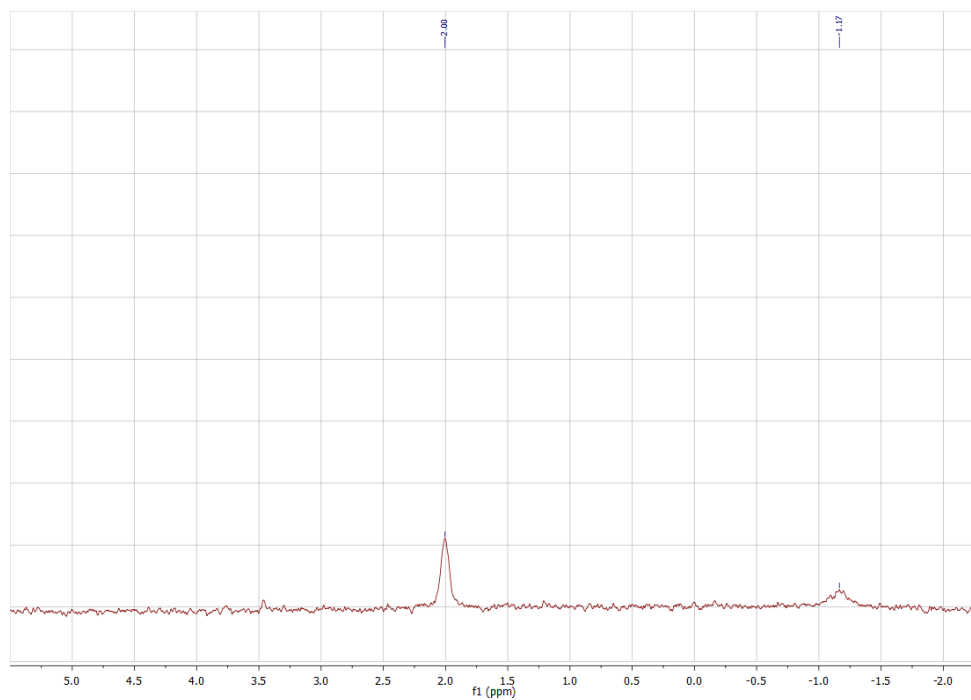


Figure S23. ^2H NMR spectrum of $4-d_5$ in THF/ C_6D_6 .

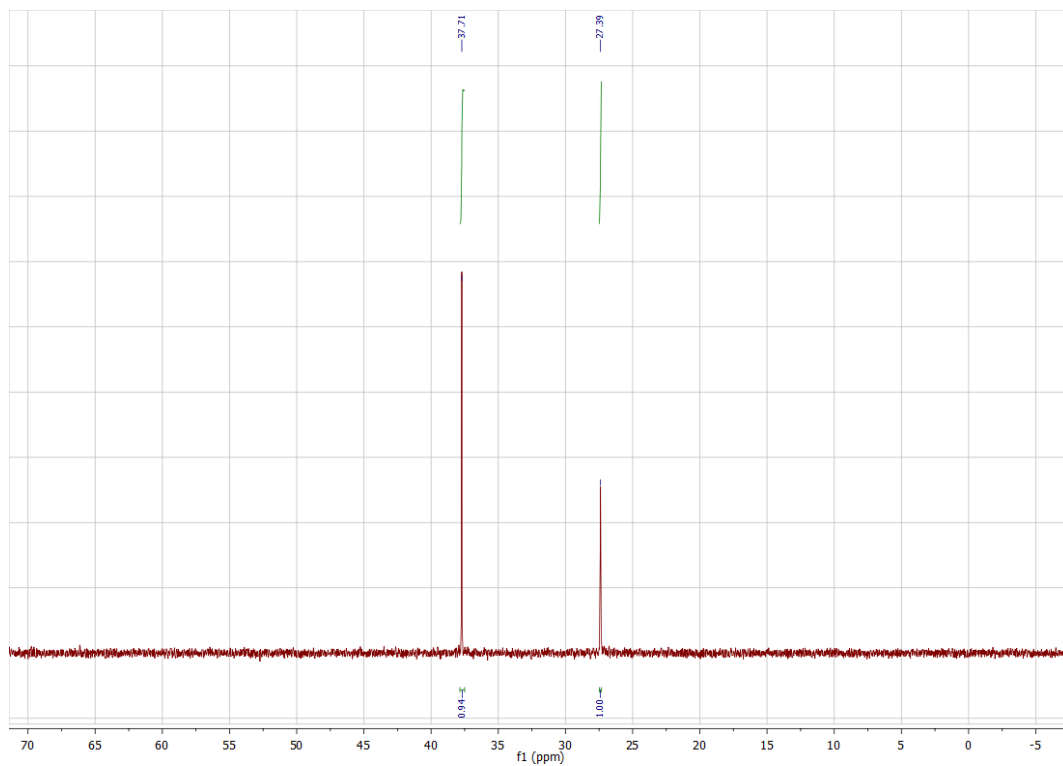


Figure S24. $^{31}\text{P}\{^1\text{H}\}$ NMR spectrum of **4-d₅** in pyridine-d₅.

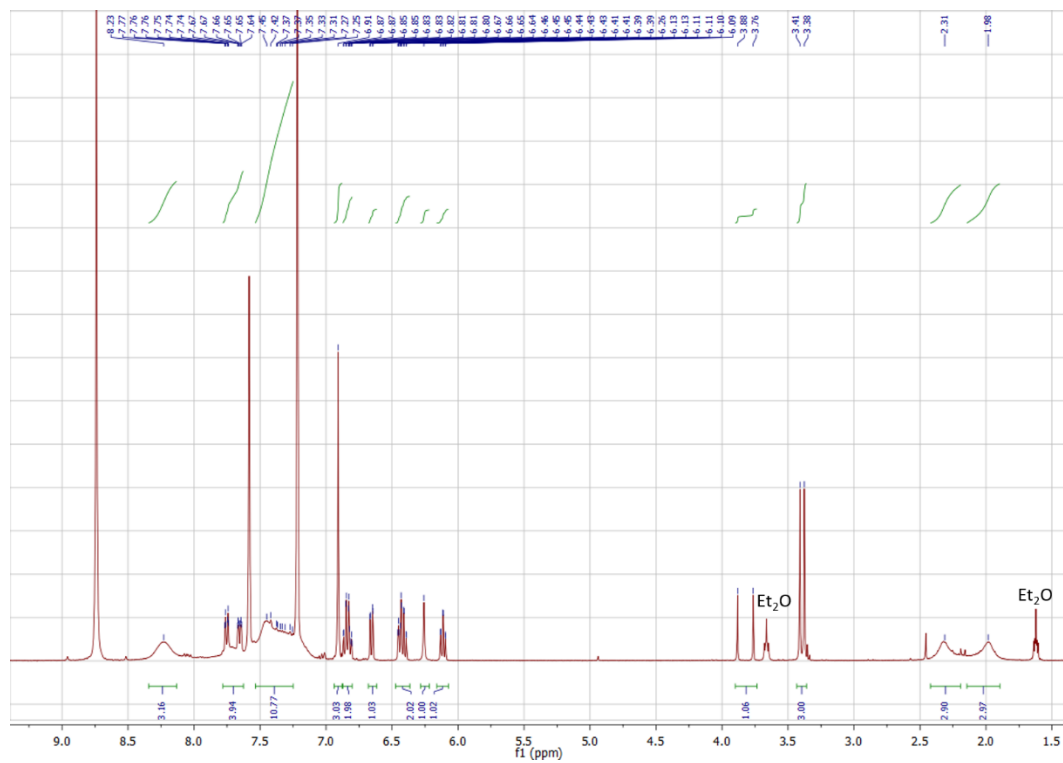


Figure S25. ^1H NMR spectrum of **5** in pyridine-d₅.

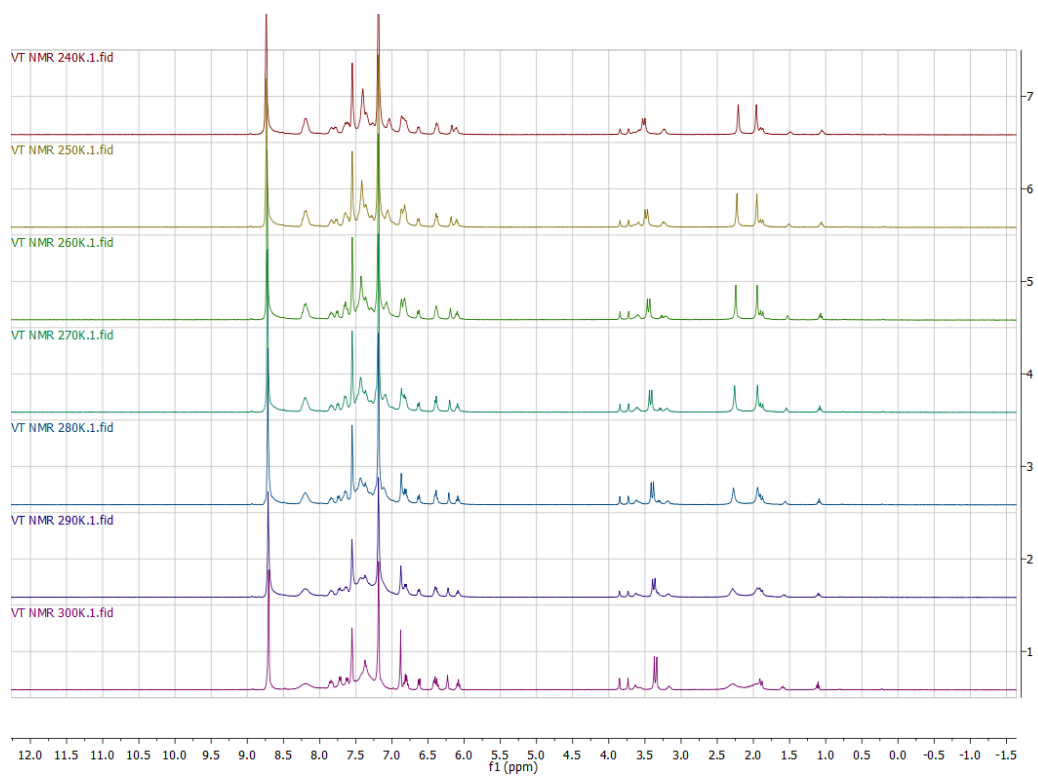


Figure S26. VT (300K to 240K) ^1H NMR spectrum of **5** in $\text{pyridine-}d_5$.

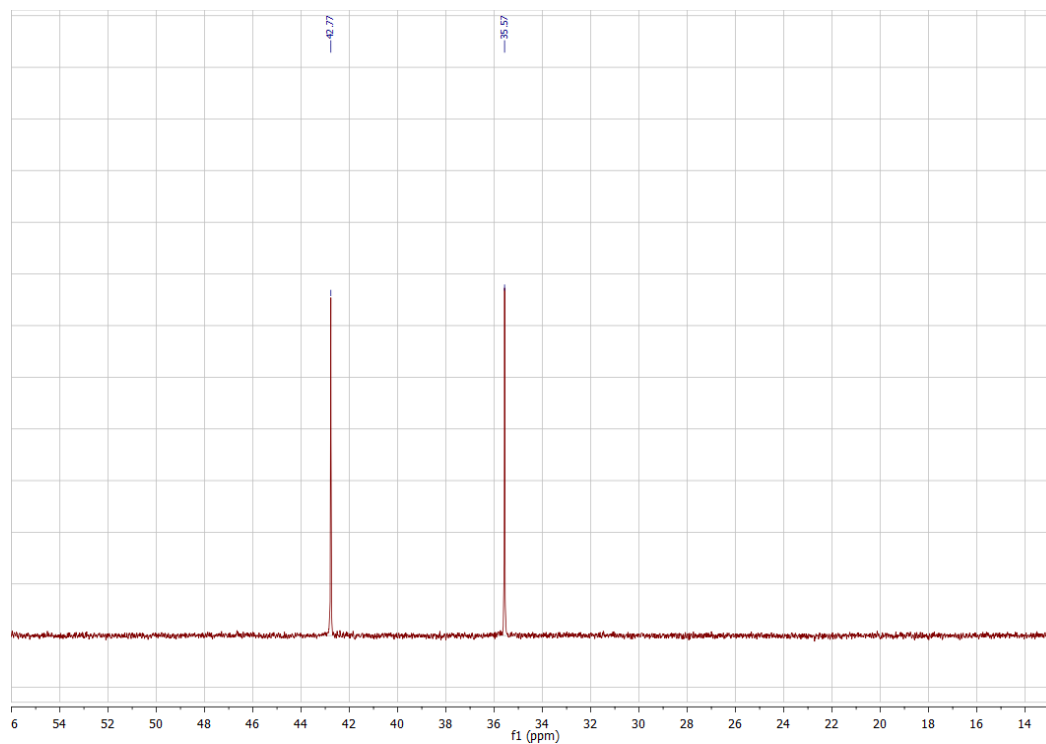


Figure S27. $^{31}\text{P}\{^1\text{H}\}$ NMR spectrum of **5** in $\text{pyridine-}d_5$.

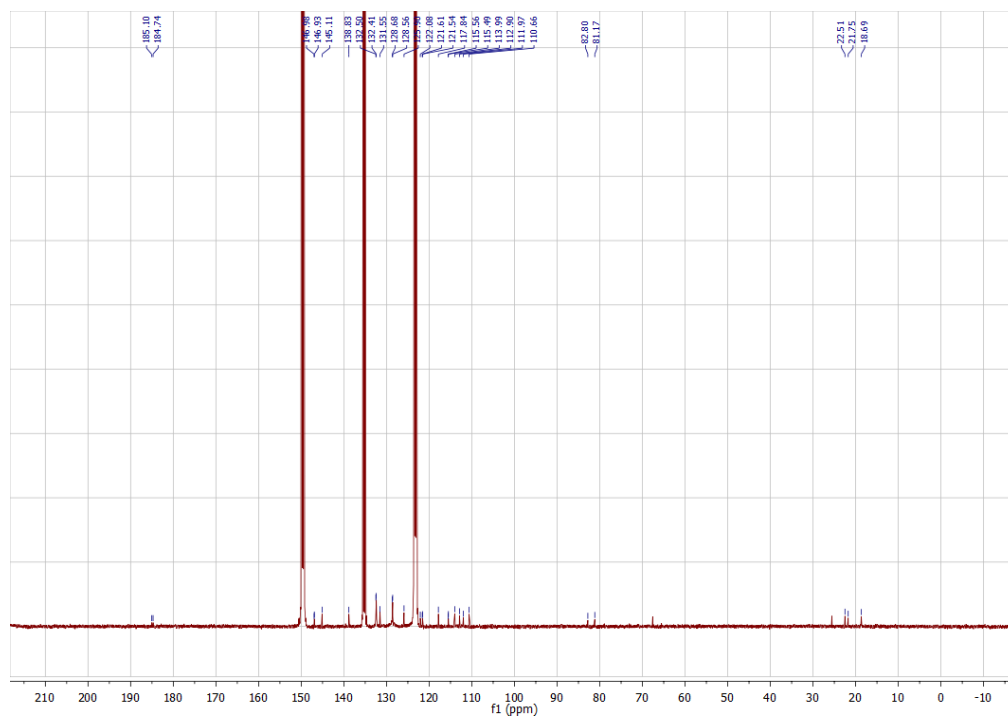


Figure S28a. $^{13}\text{C}\{^1\text{H}\}$ NMR spectrum of **5** in pyridine- d_5 .

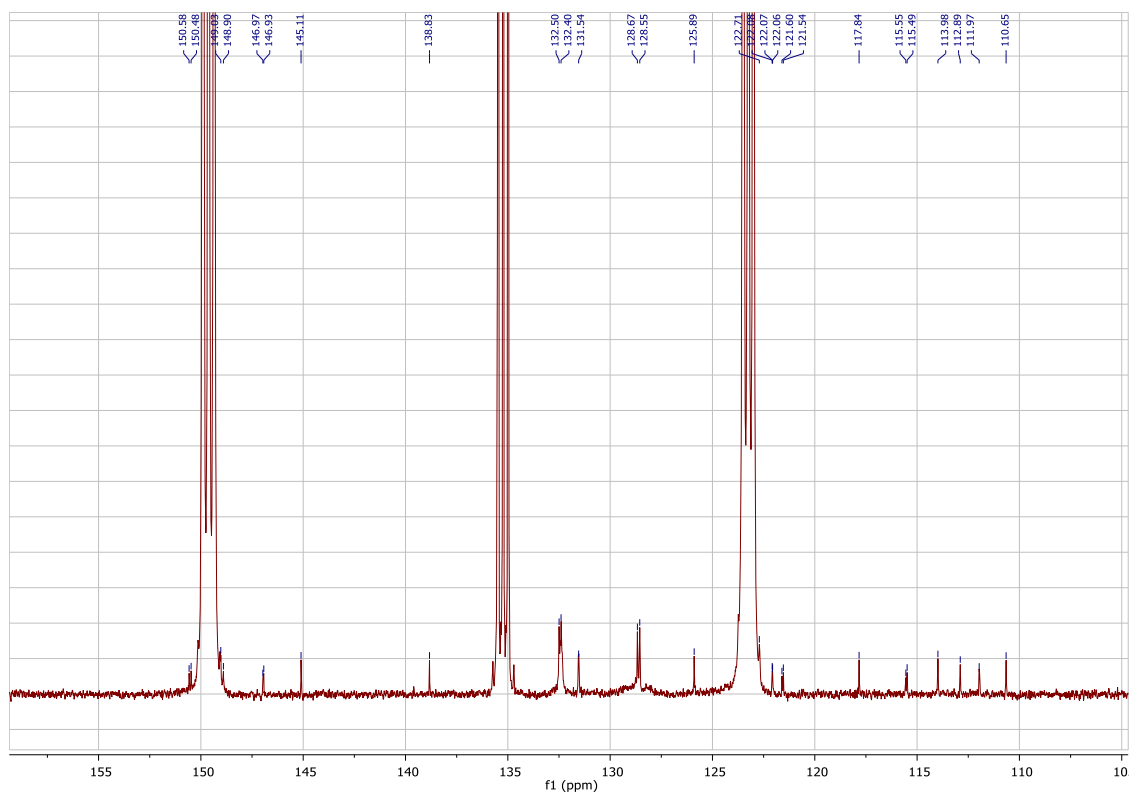


Figure S28b. $^{13}\text{C}\{^1\text{H}\}$ NMR spectrum of **5** in pyridine- d_5 from 160 to 105 ppm, see Figure S28a for the full spectrum.

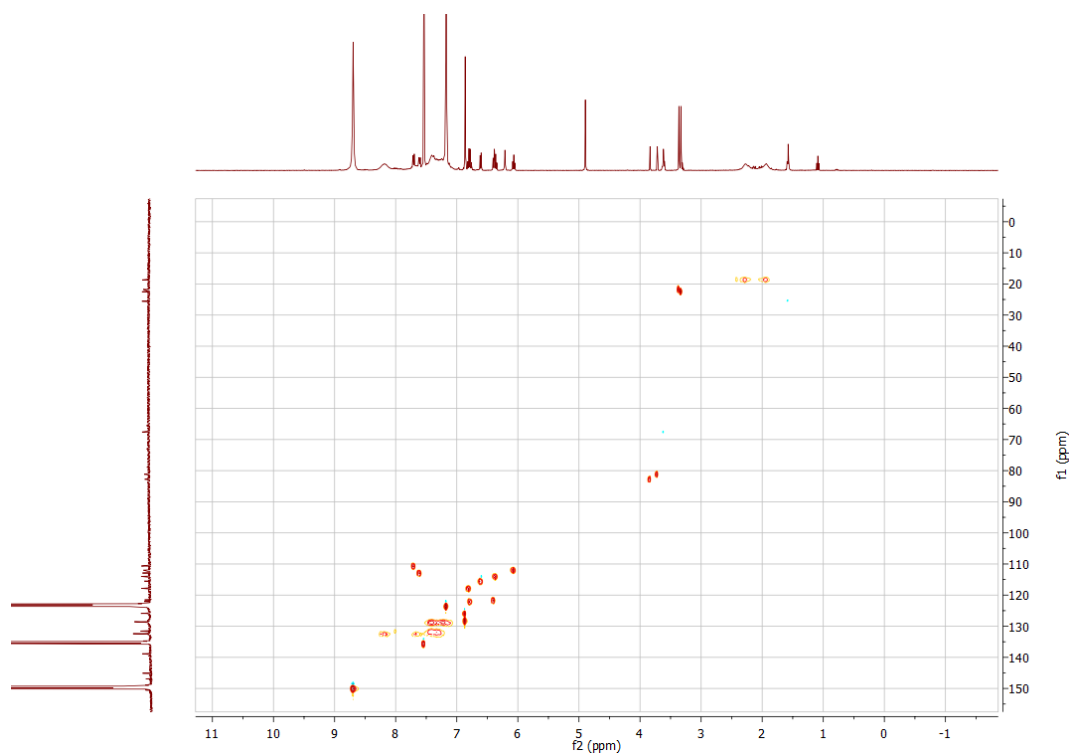


Figure S29. ^1H - ^{13}C HSQC 2D NMR spectrum of **5** in pyridine- d_5 .

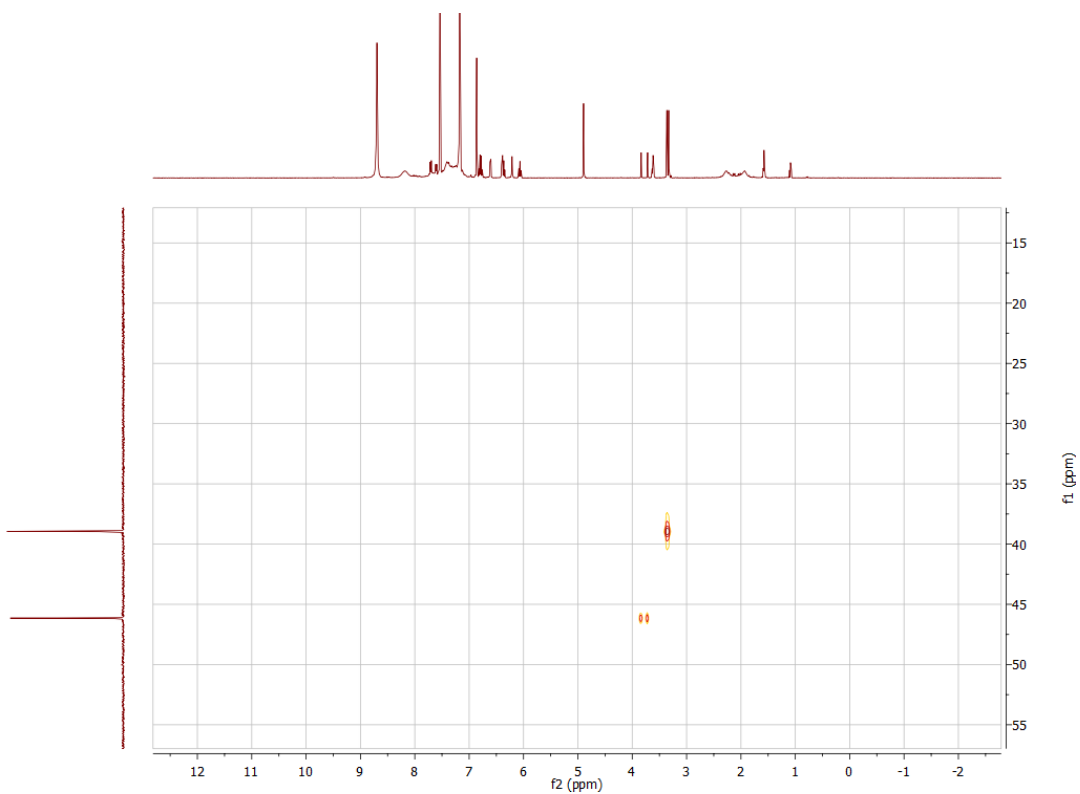


Figure S30. ^1H - ^{31}P HMBC 2D NMR spectrum of **5** in pyridine- d_5 .

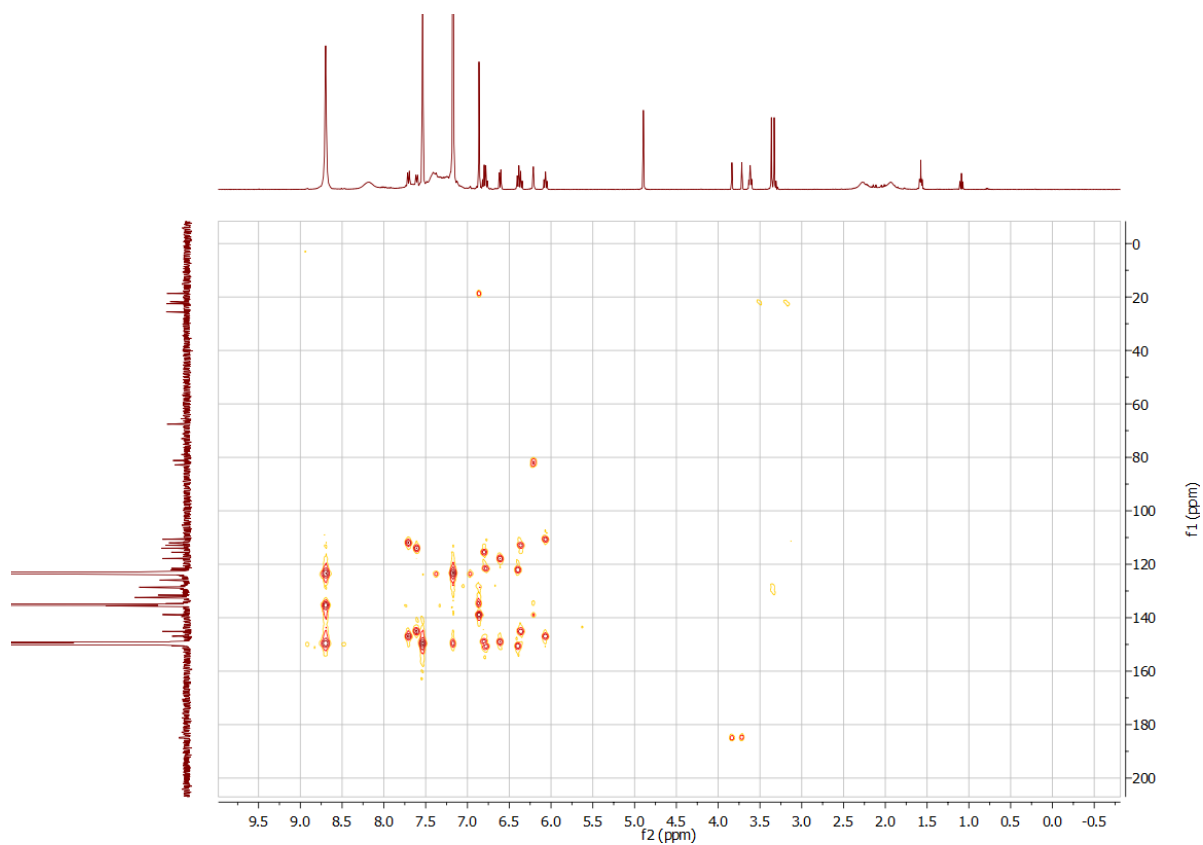


Figure S31. ^1H - ^{13}C HMBC 2D NMR spectrum of **5** in pyridine- d_5 .

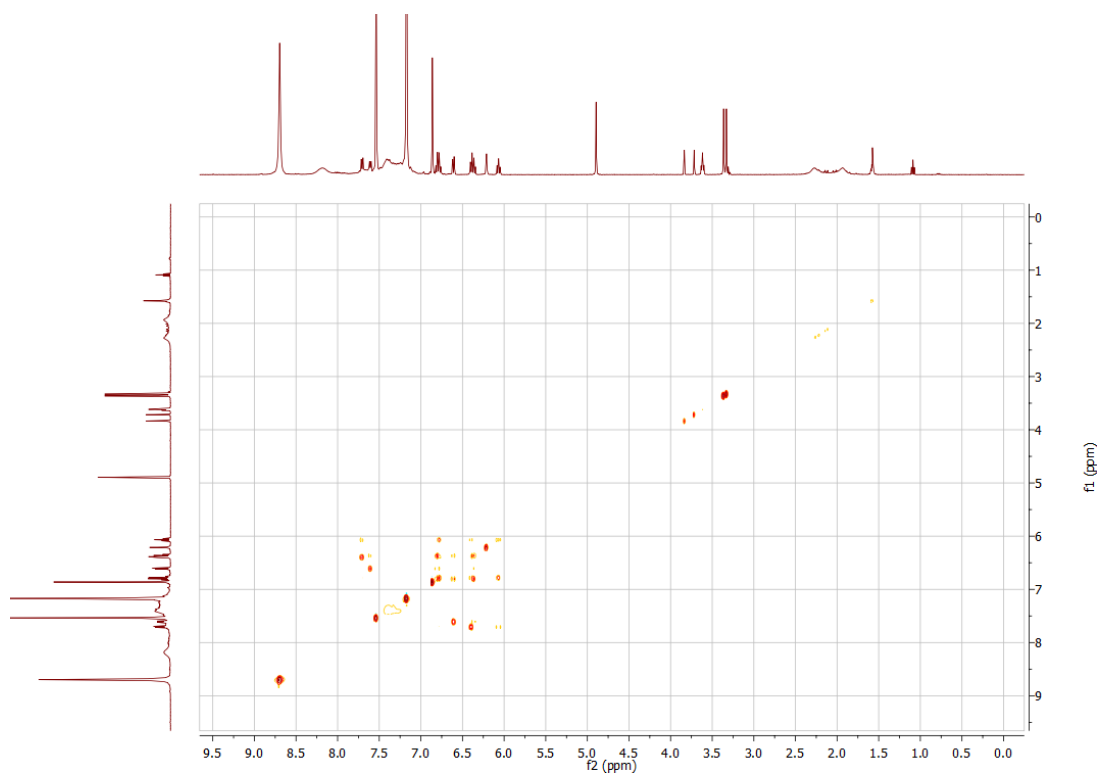


Figure S32. ^1H - ^1H TOSCY 2D NMR spectrum of **5** in pyridine- d_5 .

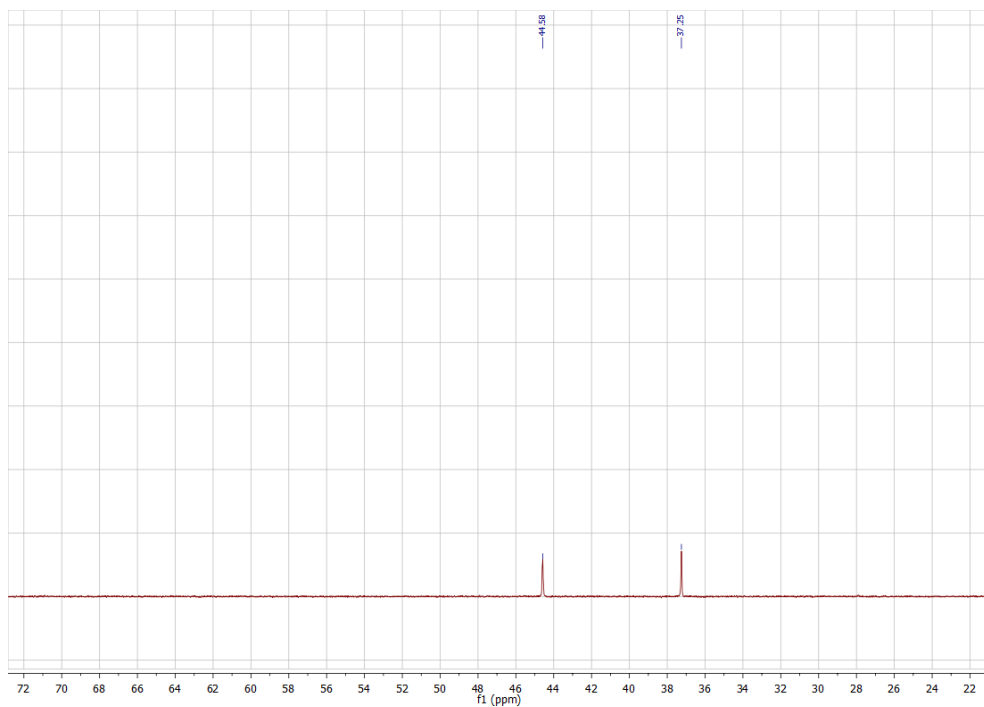


Figure S35. $^{31}\text{P}\{^1\text{H}\}$ NMR spectrum of **5-d₅** in pyridine-d₅.

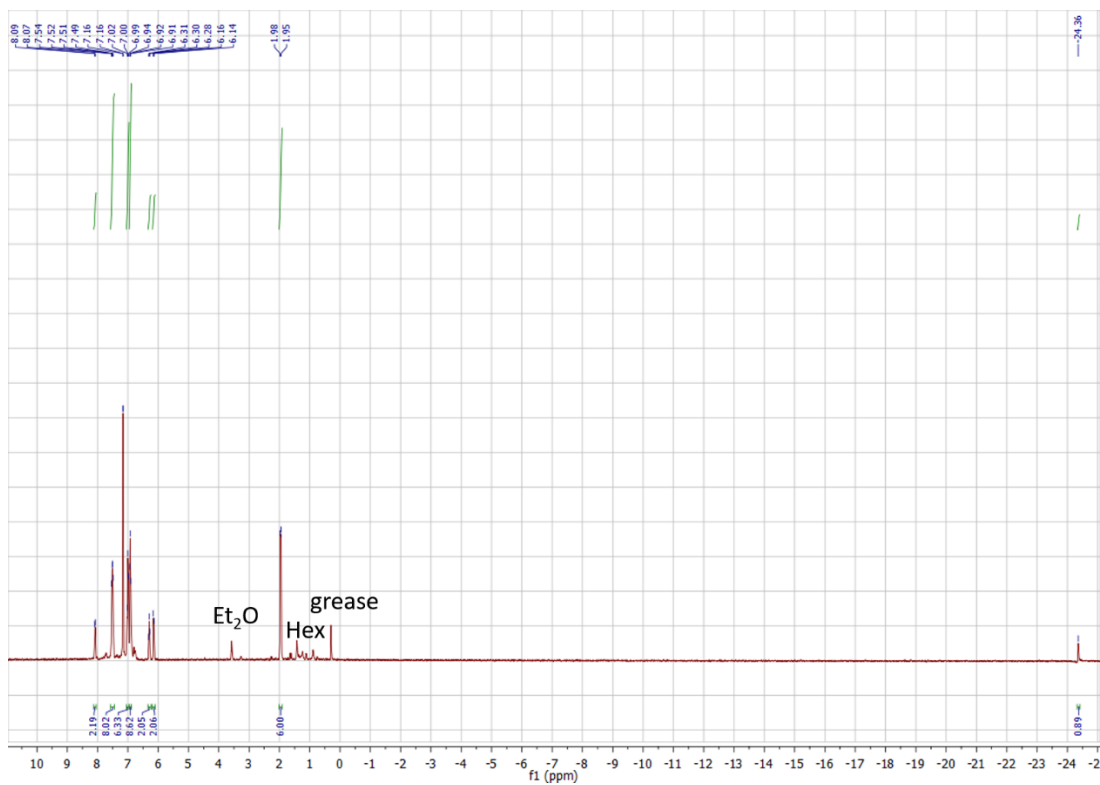


Figure S36a. ^1H NMR spectrum of **6** in C_6D_6 .

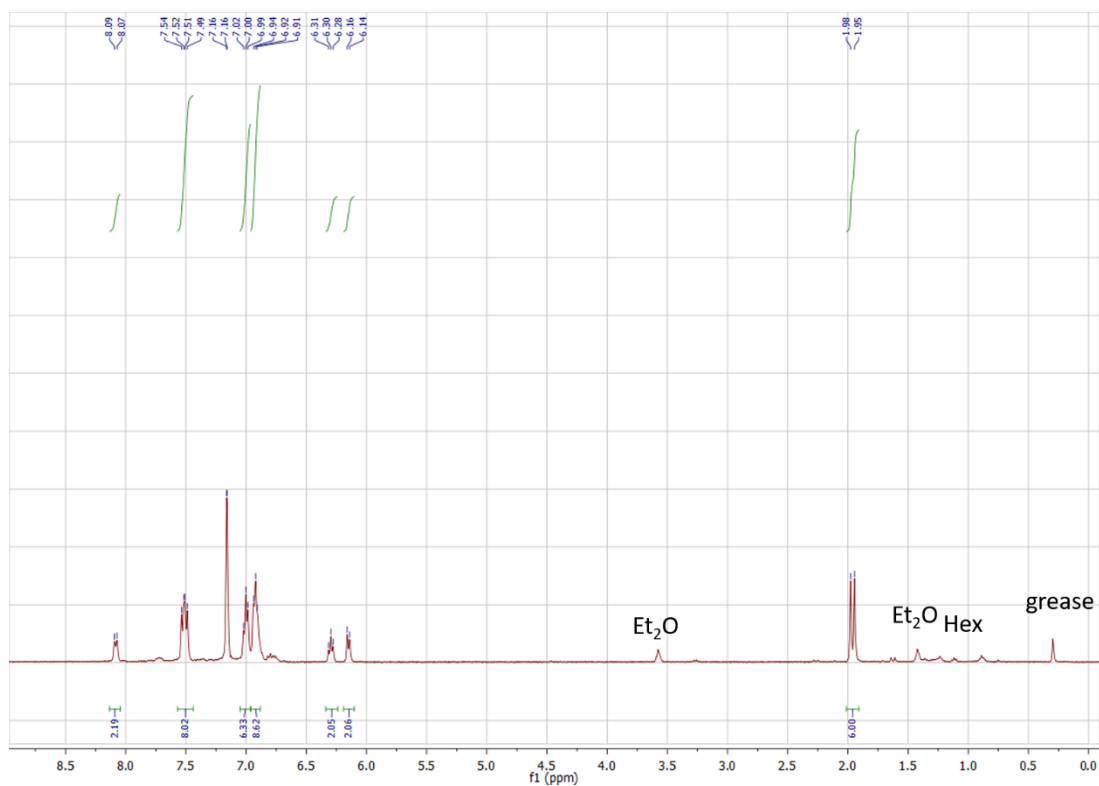


Figure S36b. ^1H NMR spectrum (0-9 ppm window) of **6** in C_6D_6 . Ni-H peak at -24.36 ppm is shown in Figure S36a.

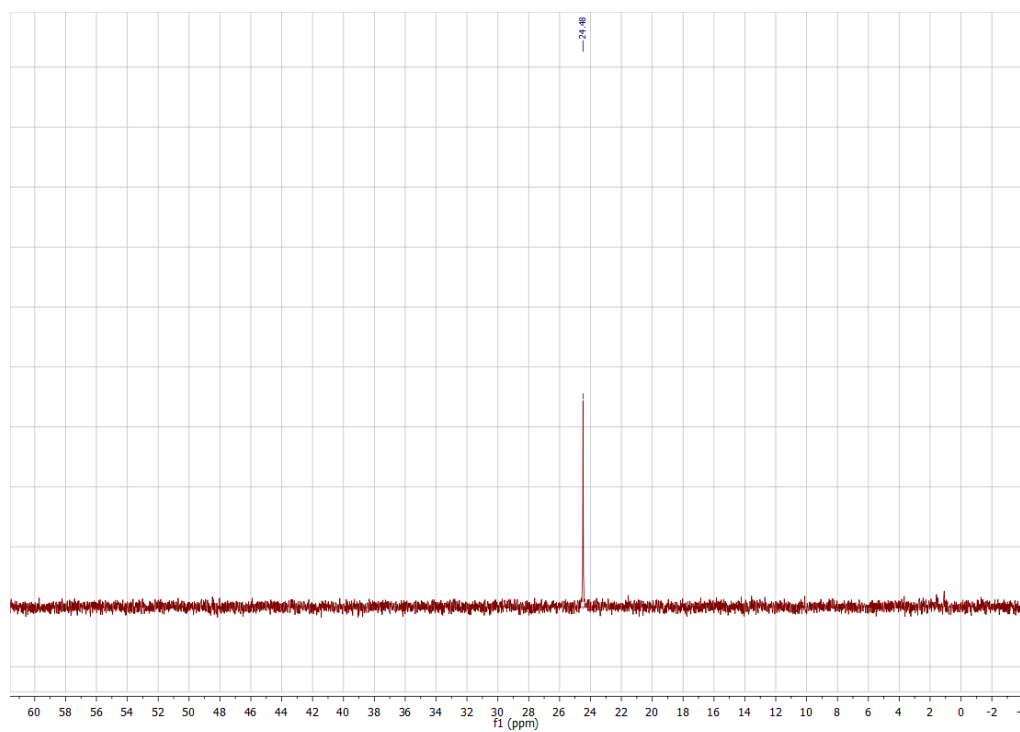


Figure S37. $^{31}\text{P}\{^1\text{H}\}$ NMR spectrum of **6** in C_6D_6 .

2. Kinetic Study of Isocyanide Insertion

2.1: Decay of **4** and **4-d₅**

All kinetic experiments were performed in J. Young NMR tubes in THF-*d*₈ and recorded on a Bruker UNI 400 NMR spectrometer at 300 K. Trimethoxybenzene was added as an internal standard. Samples were prepared by addition of 8 mg of **4** or **4-d₅** in 0.5 ml of THF-*d*₈ to a J. Young tube. ³¹P{¹H} NMR spectroscopy was used to monitor the course of the reaction. The isocyanide (2.5 equiv, 5 mg) was added to the J. Young tube (*t* = 0 min). Spectra were taken periodically and the absolute integrations were converted to concentrations.

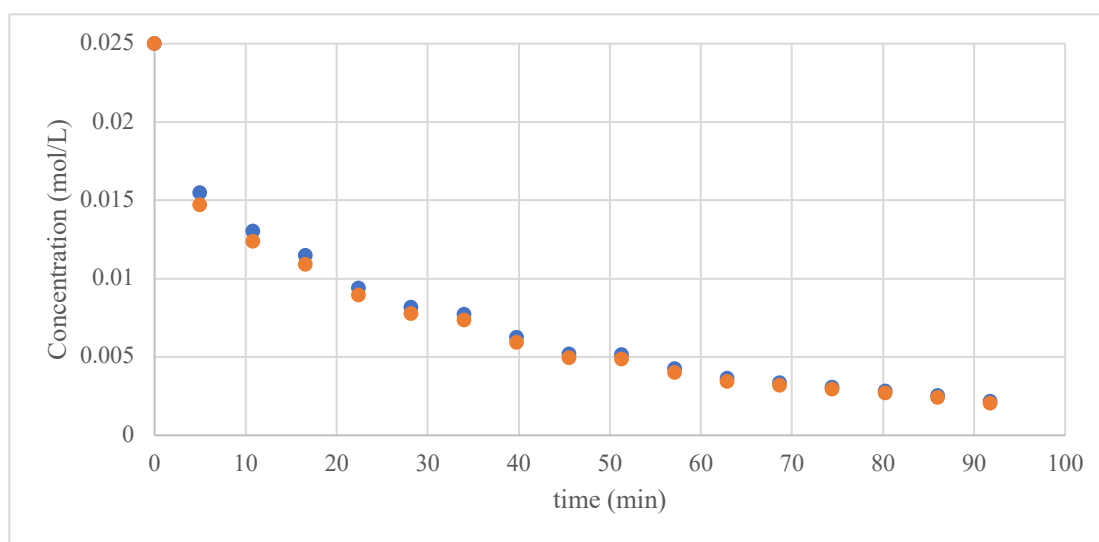


Figure S55. Plot of concentration (mol/L) of **4** (blue) and **4-d₅** (orange) vs. time (min).

Data fitting for decay of 4

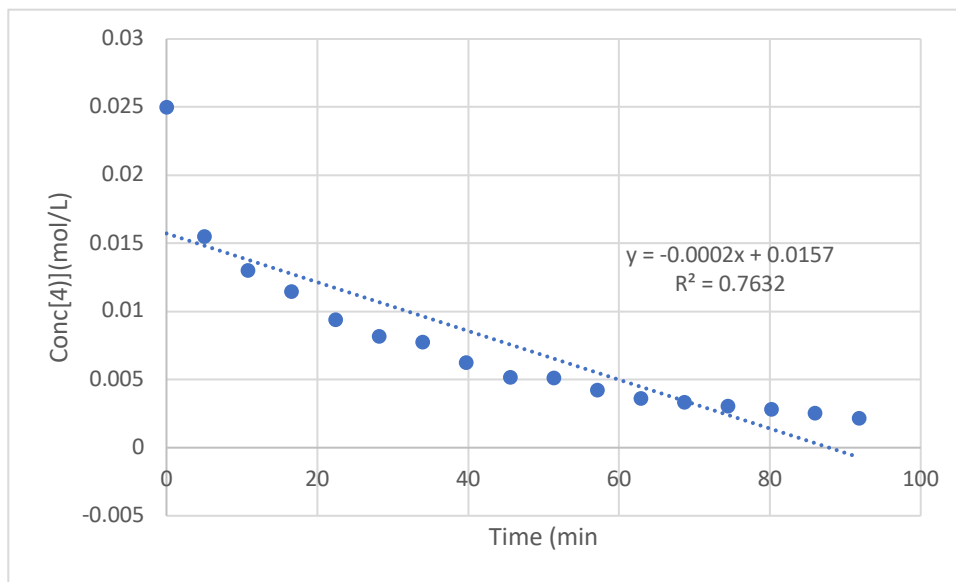


Figure S56. Plot of concentration (mol/L) of 4 vs. time (min) with 2.5 equiv of xyINC.

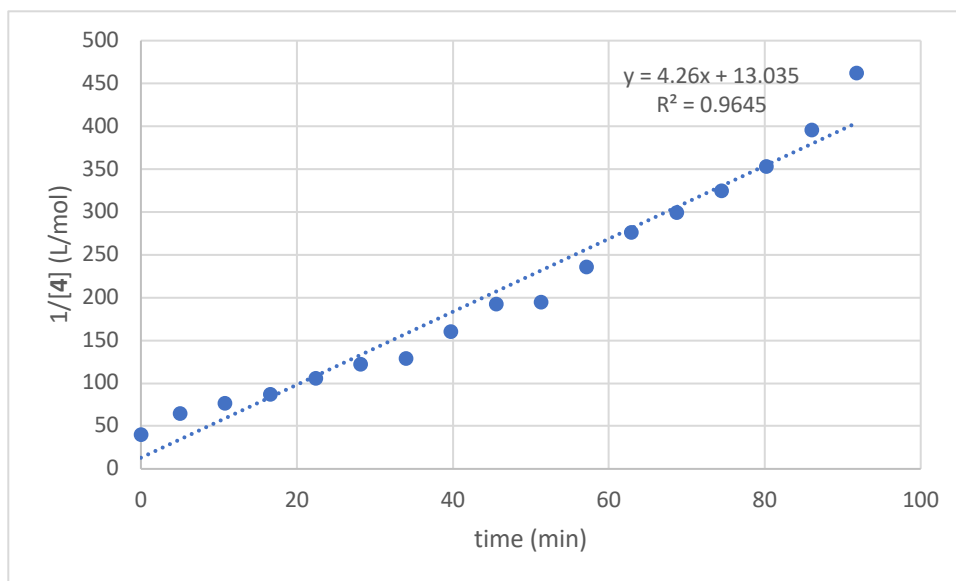


Figure S57. Plot of reciprocal of concentration of 4 vs. time (min) with 2.5 equiv of xyINC.

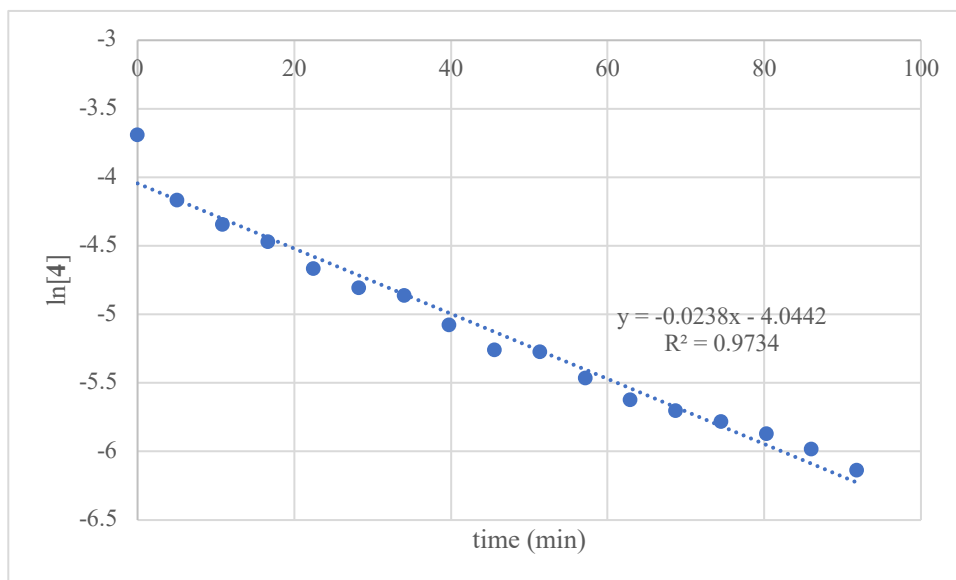


Figure S58. Plot of natural logarithm of concentration of **4** vs. time (min) with 2.5 equiv of xylNC.

Data fitting for decay of **4-d₅**

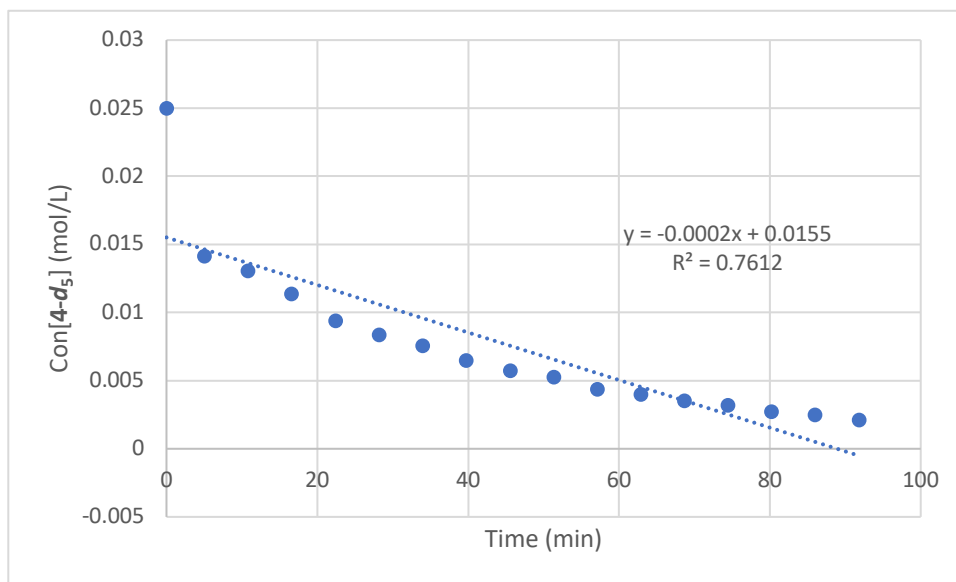


Figure S59. Plot of concentration (mol/L) of **4-d₅** vs. time (min) with 2.5 equiv of xylNC.

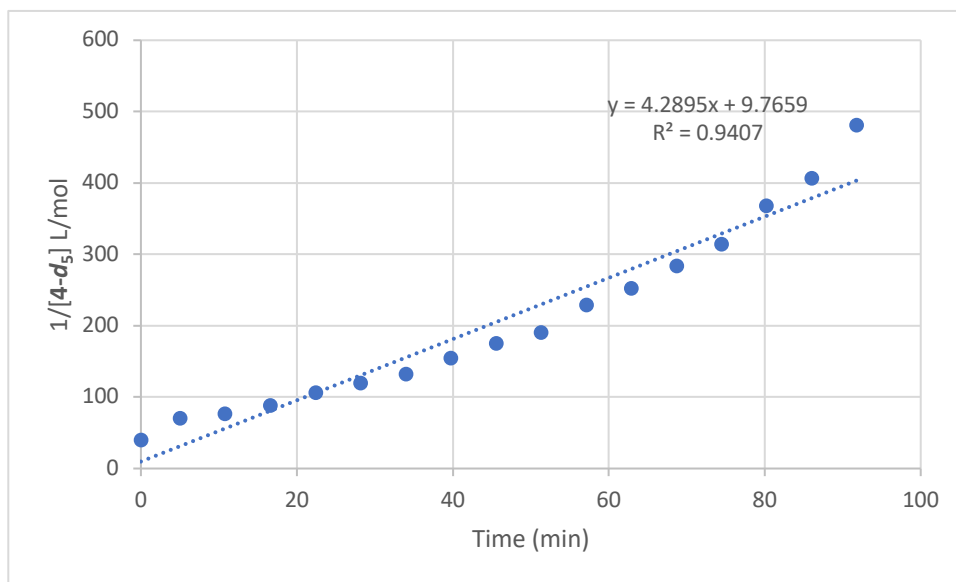


Figure S60. Plot of reciprocal of concentration of 4-d₅ vs. time (min) with 2.5 equiv of xylNC.

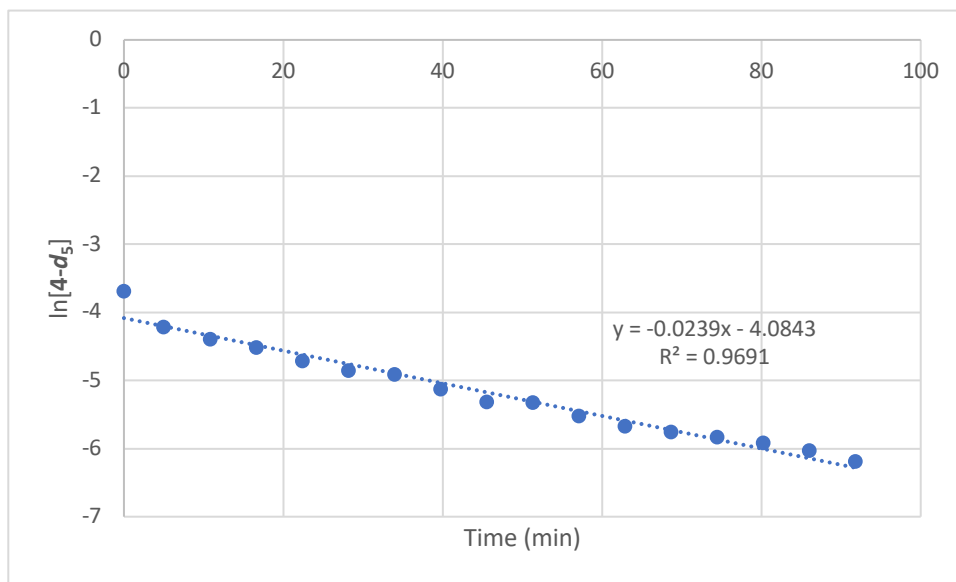


Figure S61. Plot of natural logarithm of concentration of 4-d₅ vs. time (min) with 2.5 equiv of xylNC.

2.2: Formation of **5** and **5-d₅**

For KIE studies on the formation of final product (**5**), the initial rate was recorded by plotting the concentration of formed product with time within the first 10% formation.

Table S62. Reaction rate of **4** and **4-d₅** converting to final product **5** and **5-d₅**. See below for data fitting.

	5	5-d₅	KIE
Reaction rate for formation of product (mole L ⁻¹ min ⁻¹)	1.15 x 10 ⁻⁵	2.97 x 10 ⁻⁶	3.9±0.5
Uncertainty of slope	0.05 x 10 ⁻⁵	0.23 x 10 ⁻⁶	

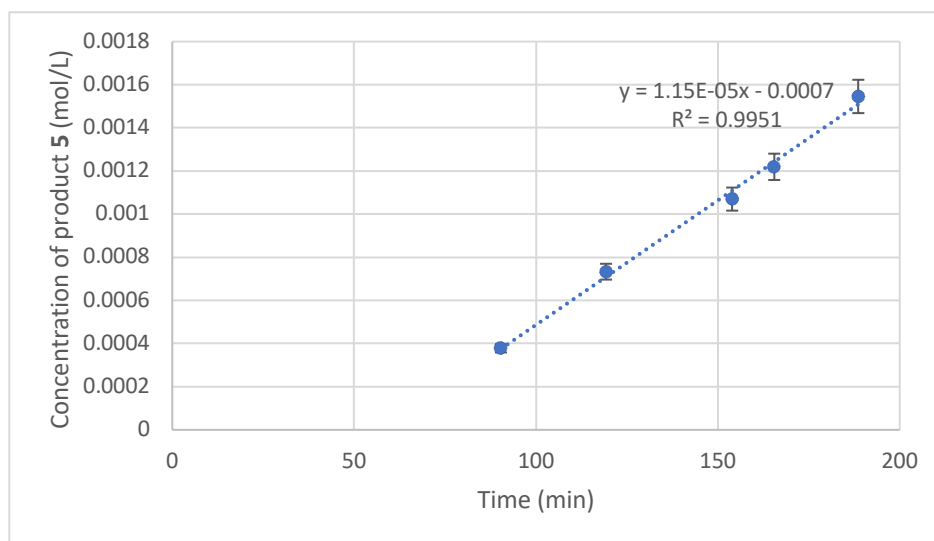


Figure S63. Plot of concentration of product **5** (mol/L) vs. time (min) in the isocyanide insertion reaction with **4**.

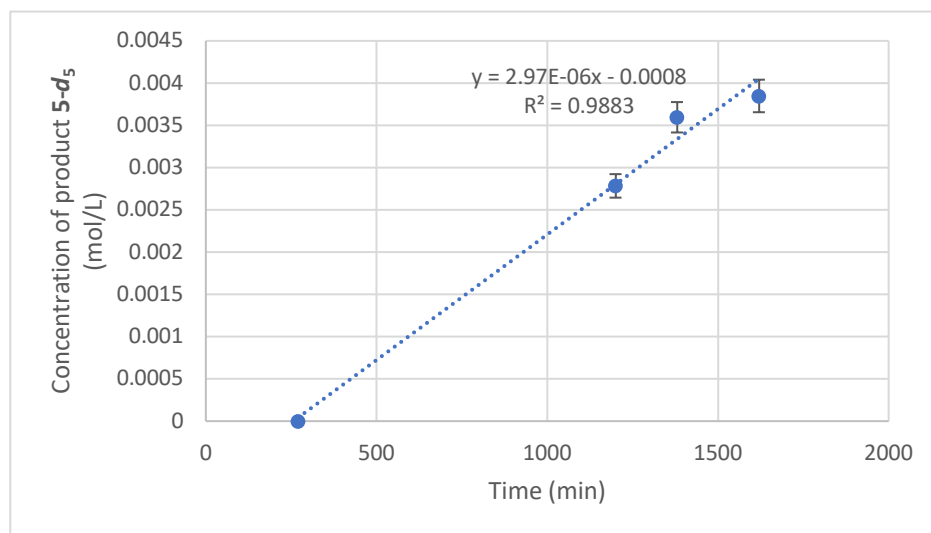


Figure S64. Plot of concentration of product (mol/L) over time (min) in the isocyanide insertion reaction with **4-d₅**.

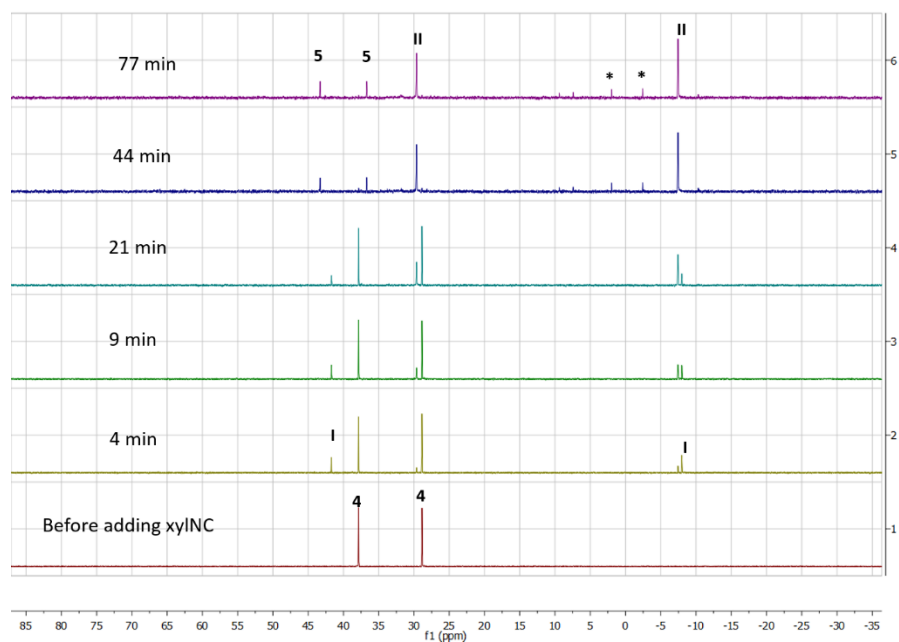


Figure S65. Selected $^{31}\text{P}\{^1\text{H}\}$ NMR spectra of the isocyanide insertion reaction with metallocycle 4 over time from $t = 0$ min to $t = 77$ min at 300K.

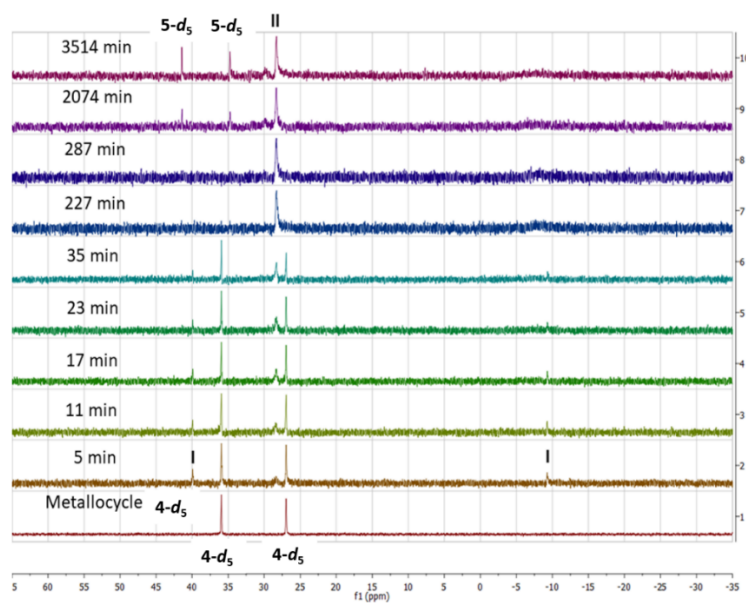


Figure S66. Selected $^{31}\text{P}\{^1\text{H}\}$ NMR spectra of the isocyanide insertion reaction with metallocycle $4-d_5$ over time from $t = 0$ min to $t = 3514$ min at 300K.

2.3: Addition of 10 equiv of xylNC

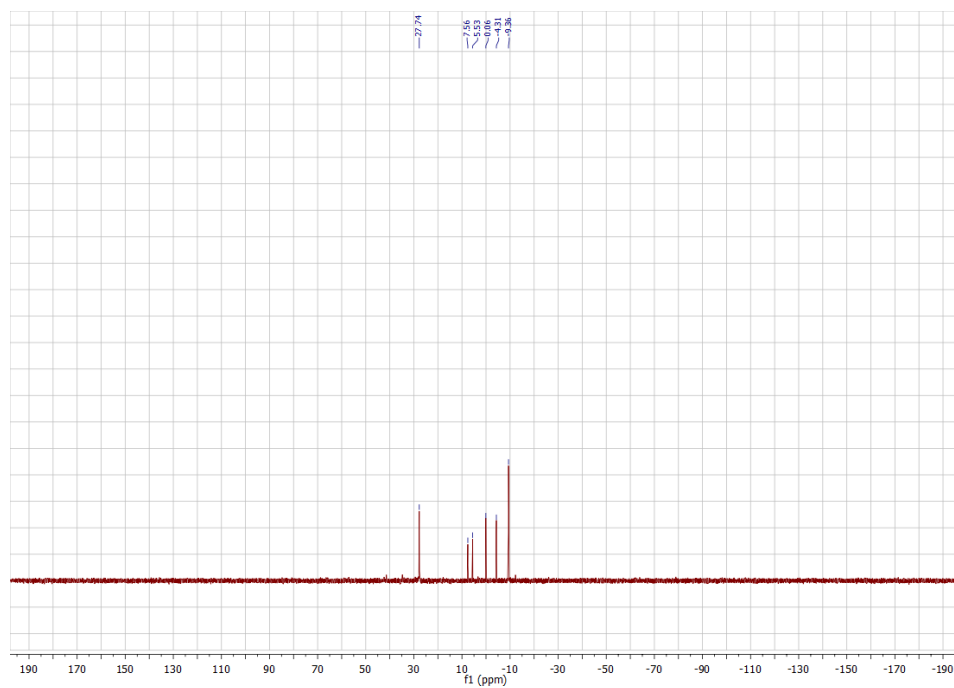


Figure S67. $^{31}\text{P}\{^1\text{H}\}$ NMR spectra of the isocyanide insertion reaction with 10 equiv of xylNC at $t = 175$ min at 300K. The identity of these species was not identified.

3. Crystallographic data

Table S68. Summary of Crystallographic data for compounds **2** and **3**

	2	3
formula	C _{51.4} H _{54.5} Cl _{0.1} N ₃ NiO _{2.9} P ₂ *	C ₄₂ H ₄₀ N ₃ NaNiOP ₂
fw	884.87	746.41
Temperature/K	100	100
Crystal system	triclinic	triclinic
space group	P-1	P-1
<i>a</i> (Å)	11.5572(6)	10.7438(3)
<i>b</i> (Å)	11.7407(6)	12.7981(4)
<i>c</i> (Å)	16.9501(8)	14.4155(5)
α (deg)	100.184(2)	69.6770(10)
β (deg)	93.978(2)	83.8800(10)
γ (deg)	102.322(2)	74.4970(10)
<i>V</i> (Å ³)	2197.81(19)	1790.91(10)
<i>Z</i>	2	2
d_{calc} (g/cm ³)	1.337	1.384
μ (mm ⁻¹)	0.567	0.682
F(000)	934.0	780.0
Crystal size, mm	0.25 × 0.23 × 0.15	0.15 × 0.13 × 0.04
2 θ range for data collection(deg)	6.428 - 55.142	5.328 - 55.102
Index ranges	-15 ≤ <i>h</i> ≤ 15, -15 ≤ <i>k</i> ≤ 15, -22 ≤ <i>l</i> ≤ 21	-13 ≤ <i>h</i> ≤ 13, -16 ≤ <i>k</i> ≤ 16, -18 ≤ <i>l</i> ≤ 16
Reflections collected	58237	48983
Independent reflections	10118[R(int) = 0.0395]	8248[R(int) = 0.0857]
Data/restraints/parameters	10118/0/561	8248/0/451
Goodness-of-fit on F ²	1.073	1.024
Final R indexes [I >= 2 σ (I)]	R ₁ = 0.0406, wR ₂ = 0.0835	R ₁ = 0.0421, wR ₂ = 0.0743
Final R indexes [all data]	R ₁ = 0.0528, wR ₂ = 0.0892	R ₁ = 0.0649, wR ₂ = 0.0815
Largest diff. peak/hole(eÅ ⁻³)	0.47/-0.41	0.46/-0.50
CCDC #	1970109	1970112

*Note: Compound 2 has 10% Cl disorder with the phenoxide in the crystal structure.

Table S69. Summary of Crystallographic data for compounds **4** and **5**

	4	5
formula	C ₄₅ H ₄₁ N ₃ NiP ₂	C ₄₉ H ₄₅ N ₅ NiP ₂
fw	744.46	824.55
Temperature/K	100	100
Crystal system	triclinic	monoclinic
space group	P-1	P2 ₁ /n
<i>a</i> (Å)	10.0629(4)	8.8277(6)
<i>b</i> (Å)	12.4737(5)	26.5464(18)
<i>c</i> (Å)	15.2136(6)	17.2437(11)
α (deg)	74.272(2)	90
β (deg)	87.324(2)	94.715(3)
γ (deg)	79.697(2)	90
<i>V</i> (Å ³)	1808.50(13)	4027.3(5)
<i>Z</i>	2	4
<i>d</i> _{calc} (g/cm ³)	1.367	1.360
μ (mm ⁻¹)	0.663	0.604
F(000)	780.0	1728.0
Crystal size, mm	0.24 × 0.07 × 0.07	0.19 × 0.09 × 0.04
2 θ range for data collection(deg)	5.806 - 55.1	5.65 - 55.124
Index ranges	-13 ≤ <i>h</i> ≤ 13, -16 ≤ <i>k</i> ≤ 16, -18 ≤ <i>l</i> ≤ 19	-11 ≤ <i>h</i> ≤ 11, -34 ≤ <i>k</i> ≤ 34, -22 ≤ <i>l</i> ≤ 22
Reflections collected	76559	114083
Independent reflections	8318[R(int) = 0.0692]	9287[R(int) = 0.1084]
Data/restraints/parameters	8318/0/462	9287/0/518
Goodness-of-fit on F ²	1.062	1.246
Final R indexes [I ≥ 2 σ (I)]	R ₁ = 0.0393, wR ₂ = 0.0819	R ₁ = 0.07456, wR ₂ = 0.1625
Final R indexes [all data]	R ₁ = 0.0537, wR ₂ = 0.0880	R ₁ = 0.0926, wR ₂ = 0.1691
Largest diff. peak/hole(eÅ ⁻³)	1.11/-0.43	0.87/-0.59
CCDC #	1970110	1970111